
Research article

The Neutrosophic Gompertz-G Family: Analytical Properties, Simulation Studies, and Applications to Real Data

Nooruldeen A. Noori^{1,*}, Mundher A. Khaleel², Tumadher M. Alharigy^{3,4}, Ehab M. Almetwally⁵ and Mohammed Elgarhy⁶

¹ Anbar Education Directorate, Anbar 31001, Iraq; Nooruldeen.a.noori35508@st.tu.edu.iq

² Department of mathematics, College of Computer Science and Mathematics, University of Tikrit, Tikrit 28001, Iraq; mun880088@tu.edu.iq

³ Department of Mathematics, Bioinformatics and Computer Applications, Maulana Azad National Institute of Technology, Bhopal 462003, India; subhankar@manit.ac.in

⁴ Department of Statistics, Faculty of Science, King Abdul Aziz University, Jeddah, Kingdom of Saudi Arabia; talharigy@kau.edu.sa

⁵ Department of Mathematics and Statistics, College of Science, Imam Mohammad Ibn Saud Islamic University (IMSIU), Riyadh 11432, Saudi Arabia; emalmetwally@imamu.edu.sa

⁶ Department of Basic Sciences, Higher Institute of Administrative Sciences, Belbeis, AlSharkia, Egypt; dr.moelgarhy@gmail.com

*Correspondence: Nooruldeen.a.noori35508@st.tu.edu.iq

ARTICLE INFO

Keywords:

Neutrosophic logic

Gompertz-G family

exponential

Mathematics Subject Classification:

62G05, 62H10, 62E10

Important Dates:

Received: 4 October 2025

Revised: 5 November 2025

Accepted: 8 November 2025

Online: 13 November 2025



Copyright © 2026 by the authors. Published under Creative Commons Attribution (CC BY) license.

ABSTRACT

This research introduces a family of continuous probability distributions based on neutrosophic logic, termed the neutrosophic Gompertz-G (NGo-G) family. The construction process begins by deriving the Gompertz-G family use the T-X transformation method, followed by its integration through the direct neutrosophic approach. The statistical properties of the proposed family are thoroughly analyzed, and applying the exponential baseline within this framework, a new model called the neutrosophic Gompertz exponential (NGoE) distribution is developed. This model includes three neutrosophic parameters and neutrosophic random variable, providing flexibility in representing uncertainty and indeterminacy. A Monte Carlo simulation is conducted to assess the efficiency and stability of the proposed estimators. The NGoE distribution is then applied to real dataset and compared with other neutrosophic models using multiple informatics criteria. The results indicate that the proposed model offers a superior fit and enhanced capability for modeling complex and imprecise data, confirming its practical relevance and statistical robustness.

1. Introduction

The T-X method proposed by Alzaatreh is a new approach to generating continuous distributions, which was developed to improve flexibility in modeling diverse data in statistics. This method is used to transform known basic distributions into new distributions that are better suited for modeling complex data, such as those that exhibit unusual properties such as skewness or kurtosis [1]. It is also a

powerful tool for generating new distributions that help improve the accuracy of data models and enhance the ability to deal with complex data that does not follow traditional distributions, examples of this method are: NKw-G Family by [2], GAEPFDs by [3], APRAY-G by [4], OLE family by [5], and NETLE by [6].

It is known that we face many skeptics regarding the classical procedures for determining the reliability of any electrical system, device, vehicle, or product in that it is (belonging, not belonging, unspecified), that is, if one of the paths of the electrical or electronic loop is unclear or not Specific, and there may be some problems related to calculating the actual probability, that is, the reliability of the system is a measure of the system's ability to work successfully under conditions and for a specific period, as with the recent development in production systems, products have become more complex in their manufacture, which increases the possibility of their collapse if one of them fails. The components in it, as one of the most important things in maintaining the reliability of the system is the use of highly reliable components, which called for finding more reliable components.

Neutrosophical logic appeared for the first time in 1995 as an extension of fuzzy logic to deal with uncertainty and inaccuracy in information. It consists of vectors or elements of true, false, and indeterminacy. The vector of the true part consists of data whose validity has been confirmed, while the false part includes data that has been verified. The unspecified part represents data whose correctness or error cannot be clearly determined. Then this logic developed to include the statistical field, and a group of neutrosophic statistical distributions emerged, including, for example: neutrosophic Lindley distribution (NLD) by [7], neutrosophic beta-Lindley distribution (NBL) by [8], NEIRD by [9], NIGD by [10], NTLEED by [11], and NIPLD by [12].

Therefore, this paper gap lies in the absence of a unified framework for generating flexible neutrosophic distribution families that combines the T-X transformation and neutrosophic logic, while integrating the neutrosophic variable into model structure and providing extensive analysis of its mathematical properties. The proposed NGo-G family aims to bridge this gap by offering a general generative model capable of representing uncertainty with higher accuracy and delivering empirical results that demonstrate its superiority over existing models.

The study aims to find a family of continuous distributions according to the T-X method and then combine it with neutrosophic logic to form a family of neutrosophic distributions with neutrosophic random variables and two neutrosophic parameters, and to prove its statistical and mathematical properties. Then to clarify the role and effect of this family, an exponential distribution according to the NGo-G family was proposed to be the NGoE distribution and obtain On the cumulative distribution, the probability density functions of the distribution, as well as the hazard functions and survival functions, drawing those functions with different periods of parameters in addition to a number of other characteristics, then estimating its parameters using the maximum likelihood method, then running a Monte Carlo simulation to find out the bias of the estimated parameters and a practical application of the knowledge. The efficiency of the proposed distribution.

The study included seven parts. The first part contained the proposed family and the method for finding it, while the second part included its statistical characteristics, while the third part contained the proposed distribution according to the generated family, while the characteristics of the proposed distribution were in the fourth part. The fifth part included estimation of the neutrosophic model parameters. The sixth part was it contains a simulation of the data generated by the model, while the seventh and final part includes a practical application to determine the efficiency of the proposed distribution.

2. Neutrosophic Gompertz-G Family

The process of deriving our family of distributions, referred to as the Neutrosophic Gompertz-G Family (NGo-G), First the Gompertz-G (Go-G) family is generated involves the following steps: Allow

$$\mathcal{P}(G) = \frac{F(x, \phi)}{1 - F(x, \phi)},$$

where $\mathcal{P}(G)$ is CDF satisfying the conditions?

- i. $\mathcal{P}(G) \in [a, b], -\infty < a < b < \infty$
- ii. $\mathcal{P}(G)$ is differentiable and monotonically non-decreasing
- ii. $\mathcal{P}(G) \rightarrow a, \text{ as } x \rightarrow -\infty, \text{ and } \mathcal{P}(G) \rightarrow b, \text{ as } x \rightarrow \infty$
- i.e. $\mathcal{P}(G) \rightarrow 0, \text{ as } x \rightarrow 0, \text{ and } \mathcal{P}(G) \rightarrow 1, \text{ as } x \rightarrow \infty$

To generate new CDF of T – X family distributions by [1]:

$$G(x, \phi) = \int_0^{\mathcal{P}(G)} m(u) du, \quad (2.1)$$

where $G(x, \phi)$ is CDF of A proposed family is, $m(u)$ is pdf of random variable $u \in [a, b]$, $\mathcal{P}(G)$ satisfy equation (2.1), take $r(x)$, $R(x)$ are pdf and CDF of Gompertz distribution respectively given by form:

$$m(x) = ae^{bx} e^{-\frac{a}{b}(e^{bx}-1)}, x > 0, a, b > 0, \quad (2.2)$$

$$\mathcal{M}(x) = 1 - e^{-\frac{a}{b}(e^{bx}-1)} \quad x > 0, a, B > 0. \quad (2.3)$$

Then the CDF of Go-G family given by:

$$G_{Go}(x, a, b, \phi) = \int_0^{\frac{F(x, \phi)}{1-F(x, \phi)}} a e^{bu} e^{-\frac{a}{b}(e^{bu}-1)} du,$$

$$G_{Go}(x, a, b, \phi) = 1 - e^{-\frac{a}{b} \left(e^{\frac{F(x, \phi)}{1-F(x, \phi)}} - 1 \right)}. \quad (2.4)$$

Or

$$G_{Go}(x, a, b, \phi) = 1 - e^{-\frac{a}{b} \left(1 - e^{-\frac{F(x, \phi)}{1-F(x, \phi)}} \right)}, \quad (2.5)$$

while pdf of Go-G family from (2.6) is:

$$g_{Go-x}(x, a, b, \phi) = \frac{af(x, \phi)}{(1 - F(x, \phi))^2} e^{\frac{F(x, \phi)}{1-F(x, \phi)}} e^{-\frac{a}{b} \left(1 - e^{-\frac{F(x, \phi)}{1-F(x, \phi)}} \right)}, \quad (2.6)$$

where $x > 0$, and a, b are shape parameters large than zero.

Definition 1 [13]: A neutrosophic number can be expressed as $X_N = X + I$, where X represents the specified component (known data) and I represents the indeterminate component (unknown data). Furthermore, X and I can represent any real integer that can be expressed as an interval with both a minimum and maximum value.

Definition 2 [13]: The collection X_N is referred to as a neutrosophic sample space when these results ensure the acquisition of the indefinite vector.

Definition 3 [13]: A subset A is considered to be derived from the sample space X_N , indicating that it belongs to the set of potential outcomes. The neutrosophic groups in sample space X_N consist of all the distinct sets, some of which may include the indeterminate vector, that serve as neutrosophic events.

Definition 4 [13-14]: Let Ω represent the sample space of a random experiment, and X_N be a designated function on Ω . The sample space of a random experiment is a comprehensive collection that encompasses all conceivable outcomes of the experiment, even those that are not explicitly described. In this particular situation, a random variable that takes on real values is symbolized as $X: \Omega \rightarrow \mathbb{R}$. Additionally, a connected random variable is symbolized as $X_N: \Omega \rightarrow \mathbb{R}(I)$, where X_N represents the Neutrosophic Random Variable and I indicates Indeterminacy. X_N is defined as the sum of X and I , specifically $X_N = X + I$.

Definition 5: Consider the neutrosophic Hybrid Inverse Rayleigh random variable, denoted as X_{Ne} , which can be expressed as $X_{Ne} = d + tI$, where d represents the determined component and tI represents the indeterminate part. The values of tI lie within the interval $[X_L, X_U]$, where X_L and X_U are the bottom and higher values of the random variable. Similarly, the values of tI are within the interval $[I_L, I_U]$. It is important to observe that the Neutrosophic Gompertz-G Family (NGo-G) becomes the classical Gompertz-G Family (NGo-G) when the lower bound (X_L) is equal to the upper bound (X_U). The Neutrosophic Cumulative Density (NCDF) of NGo-G is characterized by Neutrosophic shape parameters $a_N \in [a_L, a_U]$, $b_N \in [b_L, b_U]$, and $c_N \in [c_L, c_U]$. It may be expressed in the following form:

The Neutrosophic Gompertz-G Family (NGo-G) random variable, X_N , is defined as $X_N = d + tI$, where d represents the determined component and tI represents the indeterminate part. The values of tI are confined to the interval $[X_L, X_U]$, where X_L and X_U represent the lower and upper bounds of the random variable. Likewise, the values of tI fall within the range of $[I_L, I_U]$. It is crucial to note that the NGo-G family transforms into the classical Go-G family when the lower limit X_L is identical to the upper bound X_U . The Neutrosophic Cumulative Density (NCDF) of NGo-G is defined by the Neutrosophic shape parameters a_N , and b_N , which are within the ranges $a_N \in [a_L, a_U]$, and $b_N \in [b_L, b_U]$ respectively. The expression can be presented in the following manner:

$$G_{NGo}(x_N, a_N, b_N, \phi_N) = 1 - e^{-\frac{a_N}{b_N} \left(1 - e^{-b_N \frac{F(x_N, \phi_N)}{1-F(x_N, \phi_N)}} \right)}, \quad (2.7)$$

while Npdf of NGo-G family from (2.8) is:

$$g_{Go-x}(x_N, a_N, b_N, \phi_N) = \frac{a_N f(x_N, \phi_N)}{(1 - F(x_N, \phi_N))^2} e^{b_N \frac{F(x_N, \phi_N)}{1-F(x_N, \phi_N)}} e^{-\frac{a_N}{b_N} \left(1 - e^{-b_N \frac{F(x_N, \phi_N)}{1-F(x_N, \phi_N)}} \right)}, \quad (2.8)$$

where $f(x_N, \phi_N)$, and $F(x_N, \phi_N)$ are Npdf, and NCDF of baseline distribution with ϕ_N parameter.

Equation (2.8) defines the NCDF, which reflects how uncertainty affects the cumulative probability through the indeterminacy interval.

Proposition: Let X_N be any arbitrary random variable with NCDF $F(x_N, \phi_N)$ and Npdf $f(x_N, \phi_N)$. Also, let $U_N \in (a, b)$ be a random

variable with a pdf $r(t)$. Furthermore, let our proposed link function with NCDF and Npdf be given as:

$$\mathcal{P}(G) = \frac{F(x_N, \phi_N)}{1 - F(x_N, \phi_N)},$$

and

$$\frac{\partial \mathcal{P}(G)}{\partial x} = \frac{f(x_N, \phi_N)}{(1 - F(x_N, \phi_N))^2}.$$

The cumulative distribution function (NCDF) of the NGo-G family of distributions is expressed as:

$$G_{NGo}(x_N, a_N, b_N, \phi_N) = 1 - e^{-\frac{a_N}{b_N} \left(1 - e^{-b_N \frac{F(x_N, \phi_N)}{1 - F(x_N, \phi_N)}} \right)}.$$

Proof: Step 1: By employing the Lehman II as the Transformed (T) and the NGo-G family as the Transformer (X), we obtain:

$$G_{NGo}(x_N, a_N, b_N, \phi_N) = \int_a^{\frac{F(x_N, \phi_N)}{1 - F(x_N, \phi_N)}} \frac{a_N f(x_N, \phi_N)}{(1 - F(x_N, \phi_N))^2} e^{b_N \frac{F(x_N, \phi_N)}{1 - F(x_N, \phi_N)}} e^{-\frac{a_N}{b_N} \left(1 - e^{-b_N \frac{F(x_N, \phi_N)}{1 - F(x_N, \phi_N)}} \right)} du_N$$

$$\text{Step 2: Let } h_N = \frac{F(x_N, \phi_N)}{1 - F(x_N, \phi_N)} \Rightarrow dh_N = \frac{f(u_N, \phi_N)}{(1 - F(u_N, \phi_N))^2} du_N \Rightarrow du_N = \frac{(1 - F(u_N, \phi_N))^2}{f(u_N, \phi_N)} dh_N$$

$$G_{NGo}(x_N, a_N, b_N, \phi_N) = \int_0^{h_N} \frac{a_N f(u_N, \phi_N)}{(1 - F(u_N, \phi_N))^2} e^{b_N h_N} e^{-\frac{a_N}{b_N} (e^{b_N h_N} - 1)} \frac{(1 - F(u_N, \phi_N))^2}{f(u_N, \phi_N)} dh_N$$

$$\text{Step 3: When } u_N = 0, h_N = 0 \text{ and when } u_N = h_N, h_N = \frac{F(x_N, \phi_N)}{1 - F(x_N, \phi_N)}$$

$$G_{NGo}(x_N, a_N, b_N, \phi_N) = \int_0^{\frac{F(x_N, \phi_N)}{1 - F(x_N, \phi_N)}} e^{b_N h_N} e^{-\frac{a_N}{b_N} (e^{b_N h_N} - 1)} dh_N$$

$$G_{NGo}(x_N, a_N, b_N, \phi_N) = 1 - e^{-\frac{a_N}{b_N} \left(1 - e^{-b_N \frac{F(x_N, \phi_N)}{1 - F(x_N, \phi_N)}} \right)}$$

$$\text{Step 4: When } x_N \rightarrow 0, G_{NGo}(0, a_N, b_N, \phi_N) = 1 - e^{-\frac{a_N}{b_N} \left(1 - e^{-b_N \frac{F(0, \phi_N)}{1 - F(0, \phi_N)}} \right)} = 1 - e^{-\frac{a_N}{b_N} (e^{b_N \frac{0}{1-0}} - 1)} \\ = 1 - e^{-\frac{a_N}{b_N} (1-1)} = 1 - e^0 = 1 - 1 = 0$$

$$\text{When } x_N \rightarrow \infty, G_{NGo}(\infty, a_N, b_N, \phi_N) = 1 - e^{-\frac{a_N}{b_N} \left(1 - e^{-b_N \frac{F(\infty, \phi_N)}{1 - F(\infty, \phi_N)}} \right)} = 1 - 0 = 1$$

Step 5: Equation (2.8) is derived by differentiating $G_{NGo}(\infty, a_N, b_N, \phi_N)$ with respect to x_N , yielding the probability density function of the NGO-G family of distributions.

Sufficient evidence has been presented to establish that:

$$\int_0^\infty g_{NGo}(x_N, a_N, b_N, \phi_N) dx_N = 1,$$

$$\int_0^\infty \frac{a_N f(x_N, \phi_N)}{(1 - F(x_N, \phi_N))^2} e^{b_N \frac{F(x_N, \phi_N)}{1 - F(x_N, \phi_N)}} e^{-\frac{a_N}{b_N} \left(1 - e^{-b_N \frac{F(x_N, \phi_N)}{1 - F(x_N, \phi_N)}} \right)} dx_N = 1.$$

$$\text{Let } u_N = b_N \frac{F(x_N, \phi_N)}{1 - F(x_N, \phi_N)} \Rightarrow F(x_N, \phi_N) = \frac{u_N}{u_N + b_N} \Rightarrow 1 - F(x_N, \phi_N) = \frac{b_N}{u_N + b_N}$$

$$\text{Then } dF(x_N, \phi_N) = f(x_N, \phi_N) dx_N \Rightarrow dx_N = \frac{dF(x_N, \phi_N)}{f(x_N, \phi_N)}$$

$$\int_0^\infty g_{NGo}(x_N, a_N, b_N, \phi_N) dx_N = \int_0^\infty \frac{a_N f(x_N, \phi_N)}{\left(\frac{b_N}{u_N + b_N} \right)^2} e^{u_N} e^{-\frac{a_N}{b_N} (e^{u_N} - 1)} \frac{dF(x_N, \phi_N)}{f(x_N, \phi_N)}$$

Since $dx_N = \frac{dF(x_N, \phi_N)}{f(x_N, \phi_N)}$

$$\int_0^\infty g_{NGO}(x_N, a_N, b_N, \phi_N) dx_N = \int_0^\infty \frac{a_N(b_N + u_N)^2}{b_N^2} e^{u_N} e^{-\frac{a_N}{b_N}(e^{u_N}-1)} dx_N$$

Let $y_N = a_N e^{u_N} \Rightarrow dy_N = a_N e^{u_N} du_N \Rightarrow du_N = \frac{dy_N}{a_N e^{u_N}}$

When $u_N = 0 \Rightarrow y_N = a_N$, as $u_N \rightarrow \infty \Rightarrow y_N \rightarrow \infty$

$$\int_0^\infty \frac{a_N(b_N + u_N)^2}{b_N^2} e^{u_N} e^{-\frac{a_N}{b_N}(e^{u_N}-1)} dx_N = \int_a^\infty \frac{(b_N + u_N)^2}{b_N^2} e^{-\frac{1}{b_N}(y_N - a_N)} dy_N$$

Since $u_N = b_N \frac{F(x_N, \phi_N)}{1 - F(x_N, \phi_N)}$ Substitute these into the integral:

$$\int_0^\infty \frac{a(b + u)^2}{b^2} e^u e^{-\frac{a}{b}(e^u - 1)} dx = \frac{1}{b} \int_a^\infty e^{-\frac{1}{b}(y - a)} dy$$

$$\int_0^\infty \frac{a_N(b_N + u_N)^2}{b_N^2} e^{u_N} e^{-\frac{a_N}{b_N}(e^{u_N}-1)} dx_N = \frac{1}{b_N} \left[b_N e^{-\frac{1}{b_N}(y_N - a_N)} \right]_a^\infty = [0 + 1] = 1$$

Therefore

$$g_{NGO}(x_N, a_N, b_N, \phi_N) = \frac{a_N f(x_N, \phi_N)}{(1 - F(x_N, \phi_N))^2} e^{b_N \frac{F(x_N, \phi_N)}{1 - F(x_N, \phi_N)}} e^{\frac{a_N}{b_N} \left(1 - e^{b_N \frac{F(x_N, \phi_N)}{1 - F(x_N, \phi_N)}} \right)}$$

is Npdf function for NGo-G family.

3. Mathematical Properties of NGO-G family

5.1 Neutrosophic Survival, and Neutrosophic hazard

The Neutrosophic survival function is the probability of the system's non-failure over a given time period. The survival function is the complement of NCDF for the NGO-G family is derived using the following equation [15]:

$$S_N(x_N, a_N, b_N, \phi_N) = e^{\frac{a_N}{b_N} \left(1 - e^{b_N \frac{F(x_N, \phi_N)}{1 - F(x_N, \phi_N)}} \right)} \quad (3.1)$$

The Neutrosophic hazard function holds significant significance in numerous disciplines, including various sciences and engineering sectors, particularly in relation to matters pertaining to life. Consequently, numerous scholars have directed their efforts towards studying the hazard function and identifying statistical distributions with varying shapes for this function. As a result, the hazard function for the NGO-G family can be derived by dividing the Npdf function in equation (2.9) by the survival function in equation 10 to get the following manner [16]:

$$h_N(x_N, a_N, b_N, \phi_N) = \frac{a_N f(x_N, \phi_N)}{(1 - F(x_N, \phi_N))^2} e^{b_N \frac{F(x_N, \phi_N)}{1 - F(x_N, \phi_N)}} \quad (3.2)$$

5.2 Useful representations Npdf and NCDF of NGO-G family

The aim of this component is to improve and expand the Npdf and NCDF capability of the NGO-G family. This task requires expressing equation (2.8) using both exponential function expansion and binomial expansion. This is done taking into account the function of the NCDF distribution, which is as follows [17]:

Using exponential function expansion

$$e^{\frac{a_N}{b_N} \left(1 - e^{b_N \frac{F(x_N, \phi_N)}{1 - F(x_N, \phi_N)}} \right)} = \sum_{i=0}^{\infty} \frac{(-1)^i}{i!} \frac{a_N^i}{b_N^i} \left(1 - e^{b_N \frac{F(x_N, \phi_N)}{1 - F(x_N, \phi_N)}} \right)^i$$

Using equation (2.8), we take the term $0 < \left(1 - e^{b_N \frac{F(x_N, \phi_N)}{1 - F(x_N, \phi_N)}} \right) < 1$, and using the binomial series expansion on the last expression in the numerator of the equation as follows:

$$\left(1 - e^{b_N \frac{F(x_N, \phi_N)}{1 - F(x_N, \phi_N)}} \right)^i = \sum_{j=0}^{\infty} (-1)^j \binom{i}{j} e^{b_N j \frac{F(x_N, \phi_N)}{1 - F(x_N, \phi_N)}}$$

Then we get:

$$e^{\frac{a_N}{b_N} \left(1 - e^{b_N \frac{F(x_N, \phi_N)}{1 - F(x_N, \phi_N)}} \right)} = \sum_{i=0}^{\infty} \frac{(-1)^{i+j}}{i! b_N^i} \binom{i}{j} a_N^i e^{b_N j \frac{F(x_N, \phi_N)}{1 - F(x_N, \phi_N)}}$$

Again Using exponential function expansion, we get:

$$e^{b_N j \frac{F(x_N, \phi_N)}{1 - F(x_N, \phi_N)}} = \sum_{k=0}^{\infty} \frac{(-1)^k}{k!} b_N^k j^k F^k(x_N, \phi_N) (1 - F(x_N, \phi_N))^{-k}$$

Since $0 < (1 - F(x_N, \phi_N))^{-k} < 1$, then

$$(1 - F(x_N, \phi_N))^{-k} = \sum_{s=0}^{\infty} \frac{\Gamma(k+s)}{s! \Gamma(k)} F^s(x_N, \phi_N)$$

Then

$$e^{b_N j \frac{F(x_N, \phi_N)}{1 - F(x_N, \phi_N)}} = \sum_{k=s=0}^{\infty} \frac{(-1)^k \Gamma(k+s)}{k! s! \Gamma(k)} b_N^k j^k F^{k+s}(x_N, \phi_N)$$

Then we get:

$$e^{\frac{a_N}{b_N} \left(1 - e^{b_N \frac{F(x_N, \phi_N)}{1 - F(x_N, \phi_N)}} \right)} = \sum_{i=j=k=s=0}^{\infty} \frac{(-1)^{i+j+k} \Gamma(k+s)}{i! k! s! \Gamma(k)} \binom{i}{j} a_N^i b_N^{k-i} j^k F^{k+s}(x_N, \phi_N)$$

Finally NCDF function has the form:

$$G_{NGO}(x_N, a_N, b_N, \phi_N) = 1 - \Psi F^{k+s}(x_N, \phi_N), \quad (3.3)$$

where $\Psi = \sum_{i=j=k=s=0}^{\infty} \frac{(-1)^{i+j+k} \Gamma(k+s)}{i! k! s! \Gamma(k)} \binom{i}{j} a_N^i b_N^{k-i} j^k$

To expansion $G_{NGO}^{\delta_N}(x_N, a_N, b_N, \phi_N)$ which has the form:

$$G_{NGO}^{\delta_N}(x_N, a_N, b_N, \phi_N) = \left(1 - e^{\frac{a_N}{b_N} \left(1 - e^{b_N \frac{F(x_N, \phi_N)}{1 - F(x_N, \phi_N)}} \right)} \right)^{\delta_N}. \quad (3.4)$$

By using binomial expansion:

$$\left(1 - e^{\frac{a_N}{b_N} \left(1 - e^{b_N \frac{F(x_N, \phi_N)}{1 - F(x_N, \phi_N)}} \right)} \right)^{\delta_N} = \sum_{l=0}^{\infty} (-1)^l \binom{\delta_N}{l} e^{\frac{a_N l}{b_N} \left(1 - e^{b_N \frac{F(x_N, \phi_N)}{1 - F(x_N, \phi_N)}} \right)}.$$

By same way in NCDF expansion we get:

$$G_{NGO}^{\delta_N}(x_N, a_N, b_N, \phi_N) = T F^{z+p}(x_N, \phi_N), \quad (3.5)$$

where $T = \sum_{l=w=r=z=p=0}^{\infty} \frac{(-1)^{l+w+r+z} \Gamma(z+p)}{w! z! p! \Gamma(z)} \binom{\delta_N}{l} \binom{w}{r} a_N^w l^w b_N^{z-w} j^z$

By same way expansion Npdf function, and from NCDF expansion we get:

$$g_{NGO}(x_N, a_N, b_N, \phi_N) = \sum_{i=j=0}^{\infty} \frac{(-1)^{i+j}}{i! b_N^i} \binom{i}{j} a_N^{i+1} e^{b_N(j+1) \frac{F(x_N, \phi_N)}{1 - F(x_N, \phi_N)}} \frac{f(x_N, \phi_N)}{(1 - F(x_N, \phi_N))^2}.$$

Again Using exponential function expansion, we get:

$$e^{b_N(j+1) \frac{F(x_N, \phi_N)}{1 - F(x_N, \phi_N)}} = \sum_{t=0}^{\infty} \frac{(-1)^t}{t!} b_N^t (j+1)^t F^t(x_N, \phi_N) (1 - F(x_N, \phi_N))^{-t}$$

$$g_{NGO}(x_N, a_N, b_N, \phi_N) = \sum_{i=j=t=0}^{\infty} \frac{(-1)^{i+j+t}}{i! b_N^i t!} \binom{i}{j} a_N^{i+1} b_N^t (j+1)^t F^t(x_N, \phi_N) f(x_N, \phi_N) (1 - F(x_N, \phi_N))^{-(t+2)}$$

Since $0 < (1 - F(x_N, \phi_N))^{-(t+2)} < 1$, then

$$(1 - F(x_N, \phi_N))^{-(t+2)} = \sum_{v=0}^{\infty} \frac{\Gamma(t+2+v)}{v! \Gamma(t+2)} F^v(x_N, \phi_N)$$

Finally, the Npdf function has the form:

$$g_{NGO}(x_N, a_N, b_N, \phi_N) = Y F^{t+v}(x_N, \phi_N) f(x_N, \phi_N), \quad (3.6)$$

where $Y = \sum_{i=j=t=v=0}^{\infty} \frac{(-1)^{i+j+t} \Gamma(t+2+v)}{i! b_N^i t! v! \Gamma(t+2)} \binom{i}{j} a_N^{i+1} b_N^t (j+1)^t$

To get $g_{NGO}^{\beta_N}(x_N, a_N, b_N, \phi_N)$ which has the form:

$$g_{NGO}^{\beta_N}(x_N, a_N, b_N, \phi_N) = \frac{a_N^{\beta_N} f^{\gamma_N}(x_N, \phi_N)}{(1 - F(x_N, \phi_N))^{2\beta_N}} e^{b_N \beta_N \frac{F(x_N, \phi_N)}{1 - F(x_N, \phi_N)}} e^{\frac{a_N \beta_N}{b_N} \left(1 - e^{b_N \frac{F(x_N, \phi_N)}{1 - F(x_N, \phi_N)}}\right)}. \quad (3.7)$$

By same way in above expansion. Finally, we have the function has the form:

$$g_{NGO}^{\beta_N}(x_N, a_N, b_N, \phi_N) = E F^{m+s}(x_N, \phi_N) f^{\beta_N}(x_N, \phi_N), \quad (3.8)$$

where $E = \sum_{d=q=m=s=0}^{\infty} \frac{(-1)^{d+q+m}}{d! b_N^{d-m}} \binom{d}{q} a_N^{d+\beta_N} \beta_N^d b_N^m (q + \beta_N)^m$.

5.3 Neutrosophic Quintile function

The Neutrosophic quintile function is a mathematical function that divides a set of data into five equal halves [18]. It is the inverse of the NCDF function in equation (2.8). It also used to calculate the median, skewness, and kurtosis for distributions that have considerable skewness or lack moments. Moreover, it facilitates the development of stochastic numbers for data in simulation studies. The equation is commonly referred to as:

$$F(x_N, \phi_N) = \frac{\ln \left[1 - \frac{b_N}{a_N} \ln(1 - u_N) \right]}{b_N + \ln \left[1 - \frac{b_N}{a_N} \ln(1 - u_N) \right]}. \quad (3.9)$$

Then

$$Q_{N_{F(x_N, \phi_N)}} = Q_{u_N} \left[\frac{\ln \left[1 - \frac{b_N}{a_N} \ln(1 - u_N) \right]}{b_N + \ln \left[1 - \frac{b_N}{a_N} \ln(1 - u_N) \right]} \right]. \quad (3.10)$$

5.4 Neutrosophic Moments

Let x_N represent a Neutrosophic random variable with Npdf defined by equation (2.9). The m^{th} Neutrosophic moment of the NGo-G family distribution can be expressed as [19-20]:

$$\begin{aligned} \mu'_m &= E(x_N^m)_{NGO} = \int_0^{\infty} x_N^m g_{NGO}(x_N, a_N, b_N, \phi_N) dx_N, \\ \mu'_m &= Y \int_0^{\infty} x_N^m F^{t+v}(x_N, \phi_N) f(x_N, \phi_N) dx_N. \end{aligned} \quad (3.11)$$

5.5 Neutrosophic Moment Generating Function

The Neutrosophic moment generating function (mgf) is given by [21]:

$$M'_{x_N}(y_N)_{NGO} = E(e^{y_N x_N}) = \int_{-\infty}^{\infty} e^{y_N x_N} g_{NGO}(x_N, a_N, b_N, \phi_N) dx_N.$$

Used series expansion for $e^{y_N x_N}$

$$M'_{x_N}(y_N)_{NGO} = \sum_{m=0}^{\infty} \frac{y_N^m}{m!} E(x_N^m) = \sum_{m=0}^{\infty} \frac{y_N^m}{m!} [\mu'_m].$$

From equation (3.11) we have get:

$$M'_{x_N}(y_N)_{NGO} = \sum_{m=0}^{\infty} \frac{y_N^m}{m!} \left[Y \int_0^{\infty} x_N^m F^{t+v}(x_N, \phi_N) f(x_N, \phi_N) dx_N \right]. \quad (3.12)$$

5.6 Rényi Entropy

The Rényi entropy of the NGo-G family distribution can be derived [22]:

$$I_R(\beta_N)_{NGo} = \frac{1}{1-\beta_N} \log \int_0^\infty g_{NGo}^{\beta_N}(x_N, a_N, b_N, \phi_N) dx_N.$$

Then from equation (3.17) we have get:

$$I_R(\beta_N)_{NGo} = \frac{1}{1-\beta_N} \log \left[E \int_0^\infty F^{m+s}(x_N, \phi_N) f^{\beta_N}(x_N, \phi_N) dx_N \right]. \quad (3.13)$$

5.7 Order statistics

The Npdf of the j^{th} order statistic for a random sample of size n from a distribution function $G_{NGo}(x_N, a_N, b_N, \phi_N)$ and its related Npdf $g_{NGo}(x_N, a_N, b_N, \phi_N)$ can be expressed as [23]:

$$f_{j:n}(x) = \sum_{r=0}^{n-j} k(-1)^r \binom{n-j}{r} [G_{NGo}(x_N, a_N, b_N, \phi_N)]^{j+r-1} g_{NGo}(x_N, a_N, b_N, \phi_N). \quad (3.14)$$

4. The NGOE distribution

By using the Exponential (E) distribution as a baseline model, we can derive the Neutrosophic cumulative distribution function (NCDF) and Neutrosophic probability density function (NPDF) of the Neutrosophic Gompertz Exponential (NGOE) distribution. The NCDF is given by $F(x_N, c_N) = 1 - e^{-c_N x_N}$, while the Npdf is given by $f(x_N, c_N) = c_N e^{-c_N x_N}$ [23]. We can then substitute these equations into equation (2.8) and equation (9) to obtain the NCDF of the NGOE:

$$G_{NGOE}(x_N, a_N, b_N, c_N) = 1 - e^{\frac{a_N}{b_N} \left(1 - e^{b_N \frac{1 - e^{-c_N x_N}}{e^{-c_N x_N}}} \right)}. \quad (4.1)$$

Figure 1 shows the NCDF function of NGOE distribution with different intervals of parameters. while Figure 2 display 3D-plot of the NCDF for the NGOE distribution.

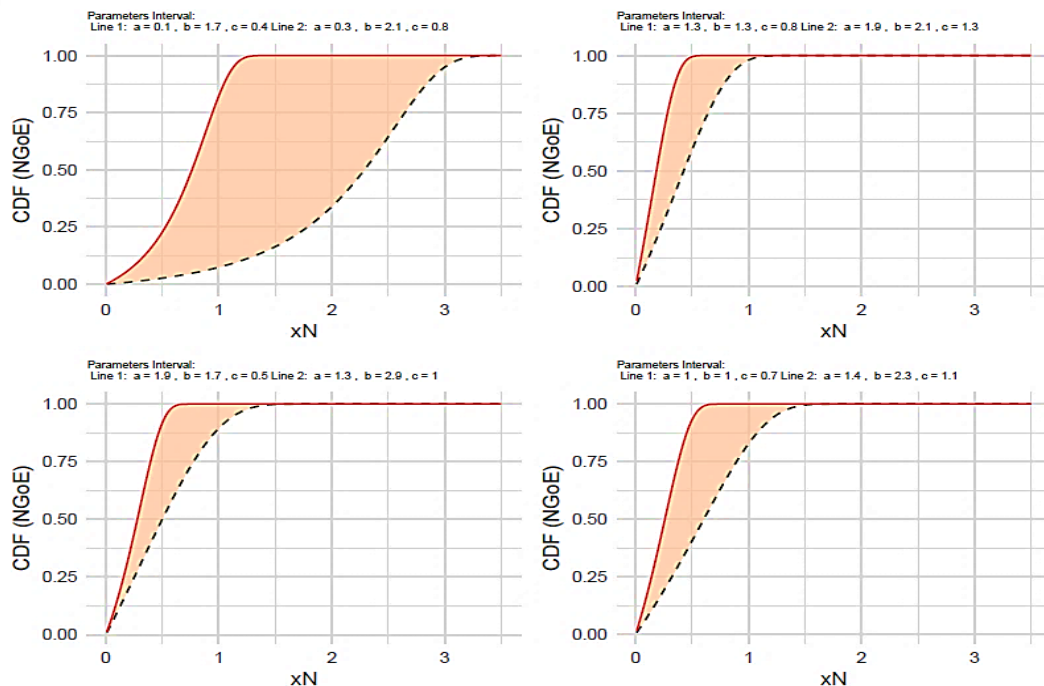


Figure 1: NCDF function of NGOE distribution with different interval of parameters

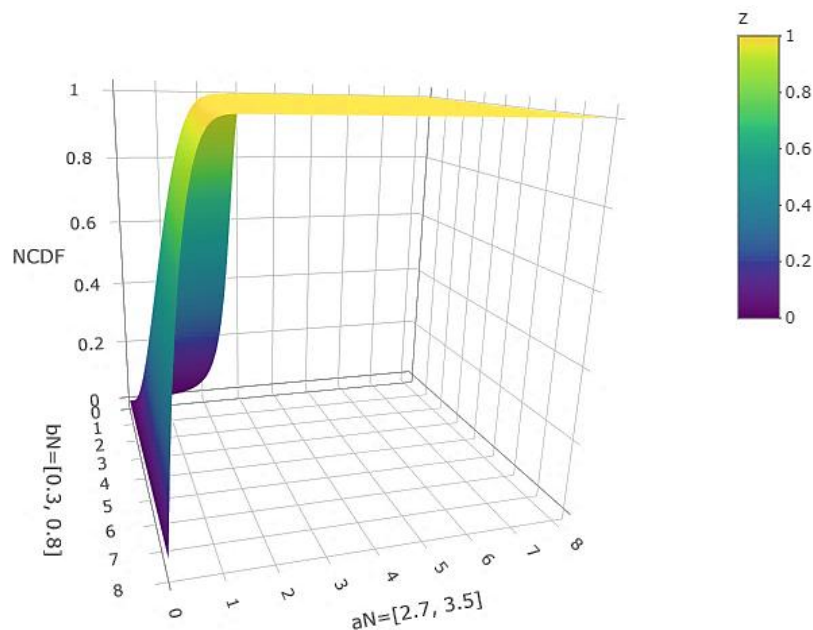


Figure 2: 3D-plot of NCDF for NGoE distribution with fixed $c_{Ne} = 0.4$

We can then substitute these equations into equation (2.9) to obtain the Npdf of the NGoE by form:

$$g_{NGoE}(x_N, a_N, b_N, \phi_N) = a_N c_N e^{-c_N x_N} e^{b_N \frac{1-e^{-c_N x_N}}{e^{-c_N x_N}}} e^{\frac{a_N}{b_N} \left(1 - e^{b_N \frac{1-e^{-c_N x_N}}{e^{-c_N x_N}}} \right)} \quad (4.2)$$

The following figure show the Npdf function of NGoE distribution with deferent intervals of parameters in Figure 3 while Figure 4 display 3D-plot of of the Npdf for the NGoE distribution.

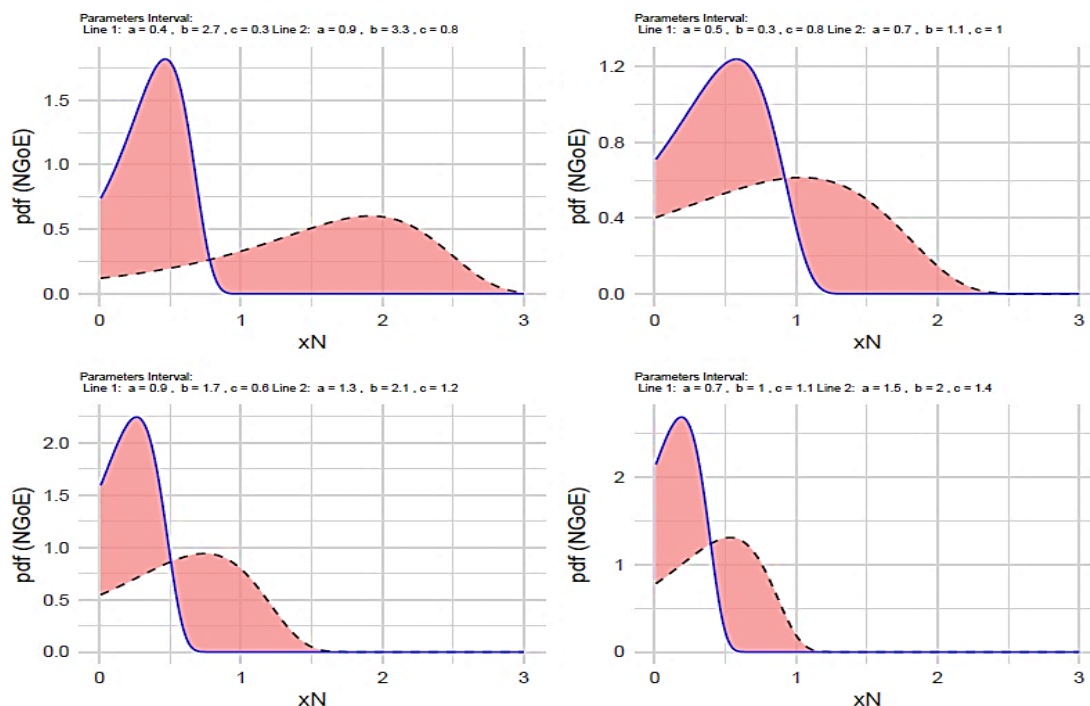


Figure 3: Npdf function of NGoE distribution with different interval of parameters

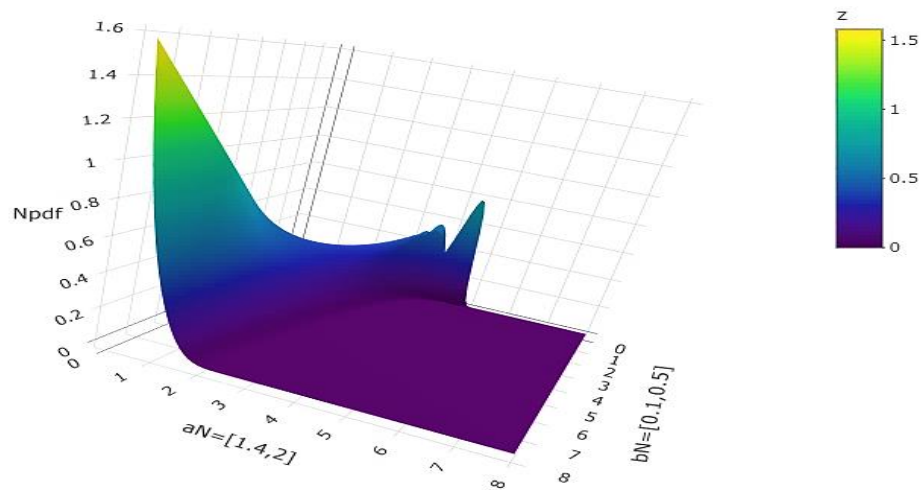


Figure 4: 3D-plot of NeCDF distribution with fixed $c_{Ne} = 0.2$

The Neutrosophic Survival function can be obtained using the following equation:

$$S_{NGoE}(x_N, a_N, b_N, c_N) = e^{\frac{a_N}{b_N} \left(1 - e^{\frac{b_N(1 - e^{-c_N x_N})}{e^{-c_N x_N}}} \right)} \quad (4.3)$$

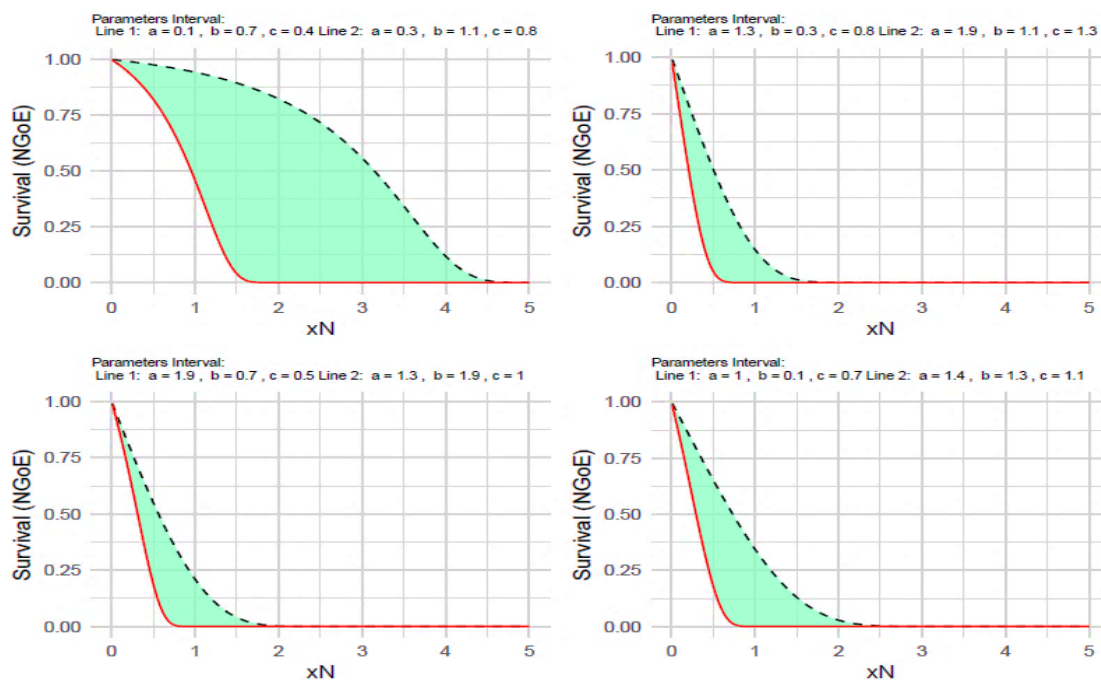


Figure 5: Neutrosophic Survival of NGoE distribution with different interval of parameters

Figure 5 presents the Neutrosophic Survival of NGoE distribution with different interval of parameters. The equation used to derive the Neutrosophic hazard functions of the NGoE distribution is:

$$h_{NGoE}(x_N, a_N, b_N, c_N) = a_N c_N e^{-c_N x_N} e^{\frac{b_N(1 - e^{-c_N x_N})}{e^{-c_N x_N}}} \quad (4.4)$$

5. Mathematical Properties of NGoE distribution

5.1 Useful representations Npdf and NCDF of NGoE distribution

The aim of this component is to improve and expand the Npdf and NCDF capability of the NGoE distribution. Then from equation (3.3) the NCDF of NGoE distribution has form:

$$G_{NGoE}(x_N, a_N, b_N, c_N) = 1 - \Psi(1 - e^{-c_N x_N})^{k_N + s_N},$$

where $\Psi = \sum_{i=j=k=s=z=0}^{\infty} \frac{(-1)^{i+j+k}\Gamma(k+s)\Gamma(k+s+z)}{i!k!s!z!\Gamma(s+2)\Gamma(k)} \binom{i}{j} a_N^i b_N^{k-i} j_N^k$

Since $0 < (1 - e^{-c_N x_N})^{k+s} < 1$, and by using binomial expansion:

$$(1 - e^{-c_N x_N})^{k+s} = \sum_{v=0}^{\infty} \frac{\Gamma(k+s+v)}{v! \Gamma(k+s)} e^{-v c_N x_N}.$$

Then the NCDF of NGOE distribution has final form:

$$G_{NGoE}(x_N, a_N, b_N, c_N) = 1 - \mathbb{H} e^{-v c_N x_N}, \quad (5.1)$$

where $\mathbb{H} = \sum_{i=j=k=s=v=0}^{\infty} \frac{(-1)^{i+j+k}\Gamma(k+s)\Gamma(k+s+v)}{i!k!s!v!\Gamma(s+2)\Gamma(k)} \binom{i}{j} a_N^i b_N^{k-i} j_N^k$

And $G_{NGoE}^{\delta_N}$ has form from equation (3.5):

$$G_{NGoE}^{\delta_N}(x_N, a_N, b_N, c_N) = T(1 - e^{-c_N x_N})^{z+p}.$$

By same way expansion NCDF function, we have get the $G_{NGoE}^{\delta_N}$ by form:

$$G_{NGoE}^{\delta_N}(x_N, a_N, b_N, c_N) = \mathcal{K} e^{-u c_N x_N}, \quad (5.2)$$

where $\mathcal{K} = \sum_{l=w=r=z=p=u=0}^{\infty} \frac{(-1)^{l+w+r+z}\Gamma(z+p)\Gamma(k+s+u)}{w!z!p!u!\Gamma(k+s)\Gamma(z)} \binom{\delta}{l} \binom{w}{r} a_N^w l_N^w b_N^{z-w} j_N^z$

By same way expansion NCDF function, the Npdf from equation (3.6) we get:

$$g_{NGoE}(x_N, a_N, b_N, c_N) = \mathcal{R} e^{-(w+1)c_N x_N}, \quad (5.3)$$

where $\mathcal{R} = \sum_{i=j=t=v=w=0}^{\infty} \frac{(-1)^{i+j+t}\Gamma(t+2+v)\Gamma(t+v+W)}{i!b_N^t t!v!W!\Gamma(t+v)\Gamma(t+2)} \binom{i}{j} c_N a_N^{i+1} (j+1)^t$

The $g_{NGoE}^{\beta_N}(x_N, a_N, b_N, c_N)$ which has the form:

$$g_{NGoE}^{\beta_N}(x_N, a_N, b_N, c_N) = \mathcal{Q} e^{-(p+\beta_N)c_N x_N}, \quad (5.4)$$

where $\mathcal{E} = \sum_{d=q=m=s=0}^{\infty} \frac{(-1)^{a+q+m}\Gamma(m+s+q)}{d! b_N^d m!q!\Gamma(m+s)} \binom{d}{q} a_N^{d+\beta_N} \beta_N^d b_N^m c_N^{\beta_N} (q + \beta_N)^m$.

5.2 Neutrosophic Quintile function

The Neutrosophic quintile function of NGOE distribution from equation (3.9) which has form:

$$x_N = -\frac{1}{c_N} \ln \left[1 - \frac{\ln \left[1 - \frac{b_N}{a_N} \ln(1 - u_N) \right]}{b_N + \ln \left[1 - \frac{b_N}{a_N} \ln(1 - u_N) \right]} \right].$$

Then

$$Q_{x_N} = Q_{u_N} \left[-\frac{1}{c_N} \ln \left[1 - \frac{\ln \left[1 - \frac{b_N}{a_N} \ln(1 - u_N) \right]}{b_N + \ln \left[1 - \frac{b_N}{a_N} \ln(1 - u_N) \right]} \right] \right]. \quad (5.5)$$

Table 1 shows the Neutrosophic quintile function values for different interval of parameters.

Table 1: Quintile function values for different intervals for a_N, b_N , and c_N

t_N	(a_N, b_N, c_N)				
	[0.2, 0.6], [0.7, 1.1], [0.8, 1.2]	[0.4, 0.8], [0.8, 1.2], [0.7, 1.3]	[0.6, 1], [0.9, 1.3], [0.4, 1.5]	[0.5, 0.7], [0.3, 1.4], [0.5, 1.3]	[0.8, 1.4], [0.6, 1.5], [0.1, 0.6]
0.1	[0.124084, 0.463103]	[0.306171, 0.088728]	[0.062777, 0.37756]	[0.37184, 0.09848]	[0.114795, 1.193416]
0.2	[0.226152, 0.751658]	[0.1658314, 0.54183]	[0.119276, 0.69558]	[0.179975, 0.6996]	[0.222635, 2.294474]
0.3	[0.313877, 0.961145]	[0.234896, 0.735220]	[0.171323, 0.97360]	[0.250326, 0.9972]	[0.32560, 3.329558]
0.4	[0.392091, 1.127582]	[0.298473, 0.901725]	[0.220368, 1.22460]	[0.31334, 1.27439]	[0.425708, 4.321516]
0.5	[0.464230, 1.268657]	[0.3586590, 1.05116]	[0.267710, 1.45835]	[0.37170, 1.53946]	[0.525018, 5.292705]
0.6	[0.533211, 1.394952]	[0.417437, 1.190792]	[0.314759, 1.68343]	[0.42770, 1.80061]	[0.626145, 6.269012]
0.7	[0.602032, 1.514569]	[0.477259, 1.327518]	[0.363345, 1.90946]	[0.483890, 2.0680]	[0.732963, 7.286920]

0.8	[0.67539,1.636411]	[0.542101,1.470593]	[0.416727,2.15125]	[0.54397,2.35901]	[0.852877,8.413282]
0.9	[0.764434,1.778355]	[0.6220166,1.64125]	[0.483454,2.44557]	[0.61734,2.71808]	[1.006169,9.828145]

5.3 Neutrosophic Moments

Let x_N represent a Neutrosophic random variable with Npdf defined by equation (2.9). The m^{th} Neutrosophic moment of the NGoE distribution from equation (3.11) and (4.2) can be expressed as:

$$\mu'_{m_N} = \mathcal{R} \int_0^{\infty} x_N^m e^{-(\mathcal{W}+1)c_N x_N} dx_N.$$

$$\text{Let } y_N = (\mathcal{W} + 1)c_N x_N \Rightarrow dy_N = (\mathcal{W} + 1)c_N dx_N \Rightarrow dx_N = \frac{dy_N}{(\mathcal{W} + 1)c_N}$$

$$\mu'_{m_N} = \mathcal{R} \int_0^{\infty} \left(\frac{y_N}{(\mathcal{W} + 1)c_N} \right)^m e^{-y_N} \frac{dy_N}{(\mathcal{W} + 1)c_N}$$

$$\mu'_{m_N} = \frac{\mathcal{R}}{((\mathcal{W} + 1)c_N)^{m+1}} \int_0^{\infty} y_N^m e^{-y_N} dy_N,$$

$$\mu'_{m_N} = \frac{\mathcal{R}\Gamma(m+1)}{((\mathcal{W} + 1)c_N)^{m+1}}. \quad (5.6)$$

Then the μ'_{1_N} , μ'_{2_N} , μ'_{3_N} , and μ'_{4_N} has forms:

$$\mu'_{1_N} = \frac{\mathcal{R}}{((\mathcal{W} + 1)c_N)^2}, \quad (5.7)$$

$$\mu'_{2_N} = \frac{2\mathcal{R}}{((\mathcal{W} + 1)c_N)^3}, \quad (5.8)$$

$$\mu'_{3_N} = \frac{6\mathcal{R}}{((\mathcal{W} + 1)c_N)^4}, \quad (5.9)$$

$$\mu'_{4_N} = \frac{24\mathcal{R}}{((\mathcal{W} + 1)c_N)^5}. \quad (5.10)$$

The Neutrosophic variance of the NGoE distribution can be calculated using the formula $\sigma_N^2 = \mu'_{2_N} - \mu'_{1_N}{}^2$ to get the form:

$$\sigma_N^2 = \frac{2\mathcal{R}}{((\mathcal{W} + 1)c_N)^3} - \frac{\mathcal{R}^2}{((\mathcal{W} + 1)c_N)^4}. \quad (5.11)$$

The Neutrosophic skewness (S) and Neutrosophic kurtosis (K) are determined by the following mathematical definitions:

$$S_N = \frac{\frac{6\mathcal{R}}{((\mathcal{W} + 1)c_N)^4}}{\left(\frac{2\mathcal{R}}{((\mathcal{W} + 1)c_N)^3} \right)^{\frac{3}{2}}}, \quad (5.12)$$

$$K_N = \frac{6(\mathcal{W} + 1)c_N}{\mathcal{R}} - 3. \quad (5.13)$$

A set of values for the intervals of Neutrosophic moments, Neutrosophic variance, Neutrosophic skewness, and Neutrosophic kurtosis are shown in Table 2.

Table 2: Numerical value of $\hat{\mu}_{1N}, \hat{\mu}_{2N}, \hat{\mu}_{3N}, \hat{\mu}_{4N}, \sigma_N^2, S_N$, and K_N of the NeHWIR distribution

KU_N	[5.401366,162.5901]	[4.084482,73.16838]	[2.89752,41.76826]	[2.33217127,46709]	[2.332171,7.671693]	[1.813244,5.842058]
SK_N	[2.262876,12.3616]	[1.969411,8.302904]	[1.661136,6.28425]	[1.490741,5.103265]	[1.339374,2.695344]	[1.302834,2.354104]
σ_N^2	[0.003706,0.089677]	[0.008258,0.107963]	[0.014537,0.127103] 	[0.022076,0.129361]	[0.068501,0.094744]	[0.080414,0.085217]
$\hat{\mu}_{4_N}$	[0.00227, 0.074463]	[0.005175,0.099908]	[0.0094,0.144007]	[0.014722,0.177949]	[0.051916,0.17802]	[0.069334, 0.168533]
$\hat{\mu}_{3_N}$	[0.002824,0.091041]	[0.006403,0.12181]	[0.011547,0.174853 	[0.017977,0.216423]	[0.063595,0.226067]	[0.084647, 0.219311]
$\hat{\mu}_{2_N}$	[0.003737,0.117414]	[0.00841,0.156398]	[0.015001,0.222935 	[0.023152,0.276228]	[0.082263,0.305415]	[0.108941, 0.30487]
$\hat{\mu}_{1_N}$	[0.005536,0.166545]	[0.012302,0.220081]	[0.021558,0.309567 	[0.032794,0.383231]	[0.117314,0.45899]	[0.154026, 0.473768]
c_N	[0.1, 0.5]	[0.2, 0.6]	[0.3, 0.7]	[0.4, 0.8]	[0.5, 0.9]	[0.6, 1]
b_N	[0.6, 0.9]		[0.8, 1.1]		[1.2, 1.6]	
a_N	[0.1, 0.4]					[0.3, 0.7]

[1.751922,4.100073]	[1.760735,3.247249]
[1.276427,1.975722]	[1.277829,1.759562]
[0.060339,0.109867]	[0.051231,0.124065]
[0.102345,0.126542]	[0.093655,0.130699,1]
[0.124074,0.177842]	[0.14153,0.158115]
[0.157993,0.268757]	[0.200622,0.230631]
[0.219374,0.456529]	[0.27669,0.423556]
[0.7, 1.1]	[0.8, 1.2]
[1.4, 1.8]	

Figure 6 presents 3D shapes of moments, skewness, and kurtosis.

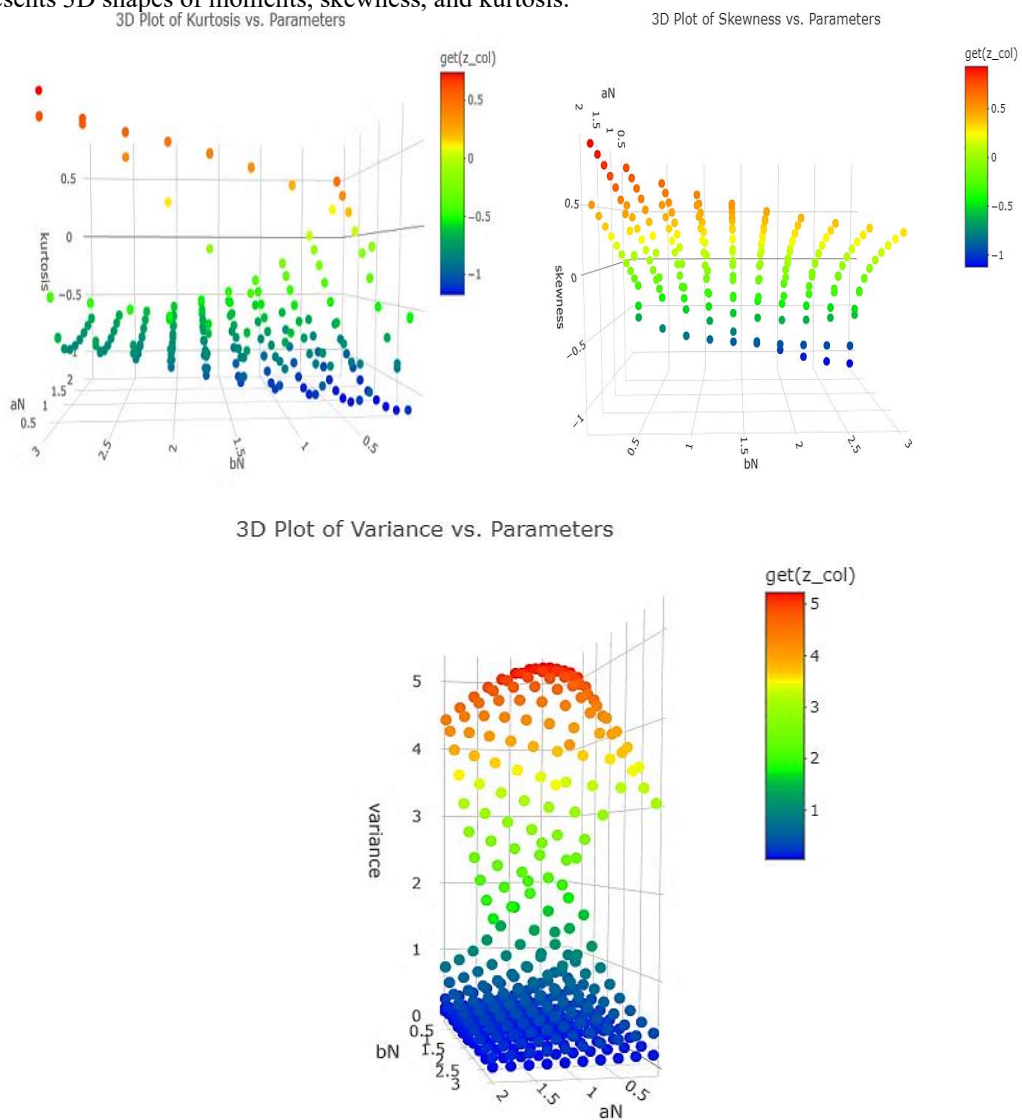


Figure 6: 3D plot of Variance, Skewness, and Kurtosis

As a function of the NGoE distribution's parameters, this image graphically depicts the dynamic behavior of three important statistical properties: variance, skewness, and kurtosis. comprehension the distribution's shape and spread requires a comprehension of

these metrics. Specifically, the graphic sheds light on the behavior of the distribution at various parameter values, demonstrating the NGoE distribution's versatility and adaptability in simulating real-world data.

The link between variance, which quantifies the spread of the data, skewness, which denotes asymmetry, and kurtosis, which quantifies the weight of the distribution's tails, is depicted in the figure using a 3D plot. One of these attributes is represented by each axis of the plot, providing a clear illustration of how changes in one feature such as skewness affect the others.

The plot probably shows that the distribution's parameters have a considerable impact on the variance, skewness, and kurtosis. Higher form parameter values, for instance, may result in a wider variance, which would suggest that the data is more dispersed. In the meantime, variations in skewness and kurtosis will indicate the degree of asymmetry in the data distribution as well as the presence of extreme values. It is possible to observe these changes simultaneously because of the comprehensive view that the 3D graphic offers.

To illustrate the behavior of the distribution under various conditions, a 3D plot is necessary. It highlights how well the NGoE distribution can describe datasets with a range of properties, including skewed or high variance data. Applications like dependability analysis and risk assessment that employ real-world data that deviates from normalcy will find this very helpful.

5.4 Neutrosophic Moment Generating Function

The Neutrosophic moment generating function (mgf) of NGoE distribution from equation (3.11) and (4.2) given by:

$$M'_{x_N}(y_N)_{NGoE} = \sum_{q=0}^{\infty} \frac{y_N^q}{q!} \left[\frac{\mathcal{R}\Gamma(m+1)}{((\mathcal{W}+1)c_N)^{m+1}} \right]. \quad (5.14)$$

5.5 Characteristic function

The NGoE distribution characteristic function can be found as follows [24]:

$$Q_{x_N}(t_N)_{NGoE} = E(e^{it_N x_N}) = \int_0^{\infty} e^{it_N x_N} g_{NGoE}(x_N, a_N, b_N, c_N) dx_N. \quad (5.15)$$

Again, applying the expansion of the exponential function and simplifying the equation based on the expansion equation we obtained the characteristic function as follows:

$$Q_{x_N}(t_N)_{NGoE} = E(e^{it_N x_N}) = \sum_{r=0}^{\infty} \frac{(it_N)^r}{r!} \left[\frac{\mathcal{R}\Gamma(m+1)}{((\mathcal{W}+1)c_N)^{m+1}} \right]. \quad (5.16)$$

5.6 Neutrosophic Incomplete Moments

The following formula can be used to find the neutrosophic incomplete moments of a random variable X_N [25]:

$$\mu'_{N_r}(y_N) = \int_0^{y_N} x_N^r g_{NGoE}(x_N, a_N, b_N, c_N) dx_N.$$

By replacing the NGoE distribution from Equation (4.2) with $g_{NGoE}(x_N, a_N, b_N, c_N)$ in the preceding equation, we obtain:

$$\mu'_{N_r}(y_N) = \mathcal{R} \int_0^{y_N} x_N^r e^{-(\mathcal{W}+1)c_N x_N} dx_N.$$

If $x_N = 0 \Rightarrow t_N = 0$, if $x_N = y_N \Rightarrow t_N = (\mathcal{W}+1)c_N y_N \Rightarrow dt_N = (\mathcal{W}+1)c_N dy_N$

Assuming the proof of Neutrosophic Moments

$$\begin{aligned} \therefore \mathcal{R} \int_0^{y_N} x_N^r e^{-(\mathcal{W}+1)c_N x_N} dx_N &= \frac{\mathcal{R}}{((\mathcal{W}+1)c_N)^{r+1}} \int_0^{\frac{t_N}{(\mathcal{W}+1)c_N}} t_N^r e^{-t_N} dt_N \\ \therefore \mathcal{R} \int_0^{y_N} x_N^r e^{-(\mathcal{W}+1)c_N x_N} dx_N &= \frac{\mathcal{R}}{((\mathcal{W}+1)c_N)^{r+1}} \Gamma\left(r+1, \frac{t_N}{(\mathcal{W}+1)c_N}\right) \end{aligned}$$

Then we have:

$$\mu'_{N_r}(y_N) = \mathcal{R}((\mathcal{W}+1)c_N)^{1-r} \Gamma\left(r+1, \frac{t_N}{(\mathcal{W}+1)c_N}\right). \quad (5.17)$$

5.7 Rényi Entropy

The Rényi entropy of the NGoE distribution can be derived.:

$$I_R(\beta_N)_{NGo} = \frac{1}{1 - \beta_N} \log \left[Q \int_0^\infty e^{-(q + \beta_N)c_N x_N} dx_N \right].$$

Then we have The Rényi entropy of the NGoE by form:

$$I_R(\beta_N)_{NGoE} = \frac{\log Q - \log[(q + \beta_N)c_N]}{1 - \beta_N}. \quad (5.18)$$

5.8 Neutrosophic Arimoto Entropy

An accurate measure of the amount of information or unpredictability in a given distribution is called arimoto entropy. The following formula is used to calculate the AEN measure:

$$\hat{A}(\beta_N)_N = \frac{\beta_N}{1 - \beta_N} \left(\left[\int_0^\infty g_{NGoE}^{\beta_N}(x_N, a_N, b_N, c_N) dx_N \right]^{\frac{1}{\beta_N}} - 1 \right).$$

Using Equation (5.18), we obtain:

$$\hat{A}(\beta_N)_N = \frac{\beta_N}{1 - \beta_N} \left(\left[\frac{Q}{(q + \beta_N)c_N} \right]^{\frac{1}{\beta_N}} - 1 \right). \quad (5.19)$$

5.9 Neutrosophic Havrda and Charvat Entropy

$$\hat{H}C(\beta_N)_N = \frac{1}{2^{1-\beta_N} - 1} \left(\left[\int_0^\infty g_{NGoE}^{\beta_N}(x_N, a_N, b_N, c_N) dx_N \right]^{\frac{1}{\beta_N}} - 1 \right).$$

Using Equation (5.18), we obtain:

$$\hat{H}C(\beta_N)_N = \frac{1}{2^{1-\beta_N} - 1} \left(\left[\frac{Q}{(q + \beta_N)c_N} \right]^{\frac{1}{\beta_N}} - 1 \right). \quad (5.20)$$

5.10 Neutrosophic Tsallis Entropy

$$\hat{T}(\beta_N)_N = \frac{1}{\beta_N - 1} \left(1 - \int_0^\infty g_{NGoE}^{\beta_N}(x_N, a_N, b_N, c_N) dx_N \right).$$

Using Equation (5.18), we obtain:

$$\hat{T}(\beta_N)_N = \frac{1}{\beta_N - 1} \left(1 - \frac{Q}{(q + \beta_N)c_N} \right). \quad (5.21)$$

5.11 Order statistics

The Npdf of the j^{th} order statistic for a random sample of size n from a distribution function $G_{NGoE}(x_N, a_N, b_N, c_N)$ and its related Npdf $g_{NGoE}(x_N, a_N, b_N, c_N)$ using Equation (3.11), and (5.18), we obtain [24]:

$$\begin{aligned} f_{j:n}(x) &= \sum_{r=0}^{n-j} k(-1)^r \binom{n-j}{r} \left[1 - e^{\frac{a_N}{b_N} \left(1 - e^{b_N \frac{1-e^{-c_N x_N}}{e^{-c_N x_N}}} \right)} \right]^{j+r-1} a_N c_N e^{-c_N x_N} e^{b_N \frac{1-e^{-c_N x_N}}{e^{-c_N x_N}}} e^{\frac{a_N}{b_N} \left(1 - e^{b_N \frac{1-e^{-c_N x_N}}{e^{-c_N x_N}}} \right)}. \end{aligned} \quad (5.22)$$

If we substitute $j = 1$ in equation (5.22), we get the smallest ordered statistic, but if we substitute $j = n$, we get the largest ordered statistic.

6. Estimation

6.1 maximum likelihood estimation (MLE)

The maximum likelihood estimation approach is used to calculate the parameters of the NGoE distribution. For a random sample of data points $x_{N1}, x_{N2}, \dots, x_{Nm}$, we compute the log-likelihood function. The distribution follows the NGoE distribution's Npdf [25-26].

$$L(\theta_N, x_N) = \prod_{i=1}^m g_{NGoE}(x_N, a_N, b_N, c_N)$$

$$L(\theta_N, x_{Ni}) = \prod_{i=1}^n a_N c_N e^{-c_N x_{Ni}} e^{b_N \frac{1-e^{-c_N x_{Ni}}}{e^{-c_N x_{Ni}}}} e^{\frac{a_N}{b_N} \left(1 - e^{b_N \frac{1-e^{-c_N x_{Ni}}}{e^{-c_N x_{Ni}}}} \right)}$$

where the distribution's parameters are θ_N . Next, the log-likelihood function L can be found as follows:

$$L = \log(a_N) + m \log(c_N) - c_N \sum_{i=1}^m x_{Ni} + b_N \sum_{i=1}^m \frac{1 - e^{-c_N x_{Ni}}}{e^{-c_N x_{Ni}}} + \frac{a_N m}{b_N} - \frac{a_N}{b_N} \sum_{i=1}^m e^{b_N \frac{1-e^{-c_N x_{Ni}}}{e^{-c_N x_{Ni}}}} \quad (6.1)$$

By partially differentiating the preceding equation with regard to the distribution parameters and solving the resulting non-linear equations for $\frac{\partial L}{\partial a_N} = \frac{\partial L}{\partial b_N} = \frac{\partial L}{\partial c_N} = 0$, one may derive MLE estimates of the parameters a_N , b_N , and c_N . Analysis was unable to produce an answer. The only way to find the solution was using numerical methods. These techniques make use of R, MAPLE, SAS, and other comparable tools.

6.2 Least square estimation

The parameters can be estimated using the Least Squares Estimation (LSE) method using the equation below [27]:

$$\varphi(a_N, b_N, c_N) = \sum_{i=1}^m \left[G_{NGoE}(x_{Ni}, a_N, b_N, c_N) - \frac{1}{n+1} \right]^2$$

$$\varphi(a_N, b_N, c_N) = \sum_{i=1}^n \left[1 - e^{\frac{a_N}{b_N} \left(1 - e^{b_N \frac{1-e^{-c_N x_{Ni}}}{e^{-c_N x_{Ni}}}} \right)} - \frac{1}{n+1} \right]^2 \quad (6.2)$$

By partially deriving the above equation for the a_N , b_N , and c_N parameters, By setting the By setting the previous equations equal to zero, we may get the Least Squares estimation.

$$\frac{\partial(\varphi(a_N, b_N, c_N))}{\partial a_N} = \frac{\partial(\varphi(a_N, b_N, c_N))}{\partial b_N} = \frac{\partial(\varphi(a_N, b_N, c_N))}{\partial c_N} = 0$$

It is seen that the equations are equal to zero. Clearly, it is impossible to obtain the closed form of the aforementioned equations, and solving them manually is a difficult task. Therefore, it is crucial to employ computer programs or numerical algorithms to determine an estimate of these parameters.

6.3 Weighted Least square estimation

The weighted least squares estimators can be obtained by the equation [28-29]:

$$W(a_N, b_N, c_N) = \sum_{i=1}^m \frac{(n+1)^2(n+2)}{i(n-i+1)} \left[G_{NGoE}(x_{Ni}, a_N, b_N, c_N) - \frac{i}{n+1} \right]^2$$

$$W(a_N, b_N, c_N) = \sum_{i=1}^m \frac{(n+1)^2(n+2)}{i(n-i+1)} \left[1 - e^{\frac{a_N}{b_N} \left(1 - e^{b_N \frac{1-e^{-c_N x_{Ni}}}{e^{-c_N x_{Ni}}}} \right)} - \frac{i}{n+1} \right]^2 \quad (6.3)$$

By partially deriving the above equation for the a_N , b_N , and c_N parameters, By setting the By setting the previous equations equal to zero.

7. Simulation

Simulation is crucial in signal processing, sophisticated analysis, and controlling air temperature. Simulation is employed in signal processing to acquire a deeper understanding of ultrasound data. In meteorology, extreme analysis use simulation tools to assess extreme estimations. Utilize various methodologies and datasets. Simulation enables scholars to gain a comprehensive understanding of the processes and characteristics specific to their respective disciplines.

The efficacy of the NGoE distribution estimators is assessed by three methods: Maximum Likelihood Estimation (MLE), Least Squares Estimation (LSE), and Weighted Least Squares Estimation (WLSE). These estimators are statistical techniques employed in a Monte Carlo simulation exercise conducted using the R programming language. The study encompasses sample sizes of 25, 50, 100, and 150. We collect a total of 1000 samples using the precise parameter values mentioned in Tables 3-4. The mean values are obtained by averaging the estimators of the model parameters. Next, the bias, mean square error (MSE), and root mean square error (RMSE) [30], [31], [32] are calculated.

Table 3: Monte Carlo simulations conducted for the NGoE distribution

		$a_N = [0.5, 0.8], \quad b_N = [1.2, 1.6], \quad c_N = [0.4, 0.7]$			
N	Est.	Est.par	MLE	LSE	WLSE
25	MEAN	\hat{a}_N	[0.36614994, 0.531451]	[0.720716, 0.9752292]	[0.59357818, 0.902638]
		\hat{b}_N	[0.5888941, 0.6010876]	[0.7357447, 0.8160255]	[0.6625972, 0.7684763]
		\hat{c}_N	[0.6538496, 1.3156817]	[0.47943103, 0.912348]	[0.49235801, 0.950705]
	MSE	\hat{a}_N	[0.08030074, 0.264115]	[0.8312616, 3.357235]	[0.21058318, 0.529614]
		\hat{b}_N	[1.0842033, 1.5464976]	[1.0432555, 1.2061477]	[0.3857676, 0.9953612]
		\hat{c}_N	[0.1037629, 0.5400434]	[0.02895572, 0.144264]	[0.02623678, 0.167013]
	RMSE	\hat{a}_N	[0.28337385, 0.5139216]	[0.9117355, 1.832276]	[0.45889343, 0.727746]
		\hat{b}_N	[1.0412508, 1.2435826]	[1.0213988, 1.0982475]	[0.6211019, 0.9976779]
		\hat{c}_N	[0.3221224, 0.7348765]	[0.17016382, 0.379821]	[0.16197773, 0.408672]
	BAIS	\hat{a}_N	[0.13385006, 0.268548]	[0.1752292, 0.220716]	[0.09357818, 0.102638]
		\hat{b}_N	[0.5989124, 1.0111059]	[0.4642553, 0.7839745]	[0.5374028, 0.8315237]
		\hat{c}_N	[0.2538496, 0.6156817]	[0.07943103, 0.212348]	[0.09235801, 0.250705]
50	MEAN	\hat{a}_N	[0.36286938, 0.52633]	[0.51674561, 0.77125]	[0.46807339, 0.71339471]
		\hat{b}_N	[0.6293723, 0.7533281]	[0.6765778, 0.8203813]	[0.6720567, 0.7852835]
		\hat{c}_N	[0.62913023, 1.2252973]	[0.49555611, 0.9328026]	[0.51817912, 0.9762004]
	MSE	\hat{a}_N	[0.05674595, 0.1567224]	[0.08008315, 0.192099]	[0.04860363, 0.15167142]
		\hat{b}_N	[1.0605917, 1.7481349]	[0.3935719, 0.9737782]	[0.4424739, 0.9232126]
		\hat{c}_N	[0.08154003, 0.4119446]	[0.02068738, 0.1109390]	[0.02623558, 0.1303220]
	RMSE	\hat{a}_N	[0.23821409, 0.3958818]	[0.28298967, 0.438291]	[0.22046231, 0.38945016]
		\hat{b}_N	[1.0298503, 1.3221705]	[0.6273531, 0.9868020]	[0.6651871, 0.9608395]
		\hat{c}_N	[0.28555215, 0.6418291]	[0.14383108, 0.3330751]	[0.16197403, 0.3610014]
	BAIS	\hat{a}_N	[0.13713062, 0.2736647]	[0.01674561, 0.028749]	[0.03192661, 0.08660529]
		\hat{b}_N	[0.5706277, 0.8466719]	[0.5234222, 0.7796187]	[0.5279433, 0.8147165]
		\hat{c}_N	[0.22913023, 0.5252973]	[0.09555611, 0.2328026]	[0.11817912, 0.2762004]
100	MEAN	\hat{a}_N	[0.40165657, 0.5720927]	[0.45631778, 0.69138324]	[0.43669864, 0.6510025]
		\hat{b}_N	[0.8507334, 0.9270386]	[0.6923947, 0.8336542]	[0.6985112, 0.9057243]
		\hat{c}_N	[0.5768035, 1.1195114]	[0.50521807, 0.9646057]	[0.52076709, 0.9834497]
	MSE	\hat{a}_N	[0.04980807, 0.1291291]	[0.02449835, 0.08475843]	[0.02329916, 0.0738190]
		\hat{b}_N	[1.3834816, 1.5265990]	[0.3945897, 0.8419299]	[0.4570450, 0.9057243]
		\hat{c}_N	[0.0634330, 0.2957645]	[0.01845406, 0.1139382]	[0.02414034, 0.1266400]
	RMSE	\hat{a}_N	[0.2231772, 0.3593454]	[0.15651948, 0.29113300]	[0.15264064, 0.2716965]
		\hat{b}_N	[1.1762149, 1.2355562]	[0.6281637, 0.9175674]	[0.6760510, 0.9516955]
		\hat{c}_N	[0.2518591, 0.5438423]	[0.13584573, 0.3375473]	[0.15537161, 0.3558652]
	BAIS	\hat{a}_N	[0.09834343, 0.2279073]	[0.04368222, 0.10861676]	[0.06330136, 0.148997]
		\hat{b}_N	[0.3492666, 0.6729614]	[0.5076053, 0.7663458]	[0.5014888, 0.9516955]
		\hat{c}_N	[0.1768035, 0.4195114]	[0.10521807, 0.2646057]	[0.12076709, 0.2834497]
150	MEAN	\hat{a}_N	[0.41371647, 0.6140256]	[0.42467084, 0.67977454]	[0.42398435, 0.6511098]
		\hat{b}_N	[0.9595925, 1.1082239]	[0.7104504, 0.8548513]	[0.7858049, 0.9213440]
		\hat{c}_N	[0.55611472, 1.0649140]	[0.51654981, 0.95334547]	[0.51588814, 0.9634528]
	MSE	\hat{a}_N	[0.05061071, 0.1454143]	[0.02044684, 0.06065964]	[0.02154149, 0.0570997]
		\hat{b}_N	[1.3648510, 2.5834357]	[0.4090814, 0.9636503]	[0.5017551, 0.8773367]
		\hat{c}_N	[0.05740013, 0.2507331]	[0.02124183, 0.09977889]	[0.02471743, 0.1124012]
	RMSE	\hat{a}_N	[0.22496825, 0.3813323]	[0.14299246, 0.24629179]	[0.14677020, 0.2389554]
		\hat{b}_N	[1.1682684, 1.6073070]	[0.6395947, 0.9816569]	[0.7083467, 0.9366625]
		\hat{c}_N	[0.23958324, 0.5007326]	[0.14574576, 0.31587797]	[0.15721778, 0.3352629]
	BAIS	\hat{a}_N	[0.08628353, 0.1859744]	[0.07532916, 0.12022546]	[0.07601565, 0.1488902]
		\hat{b}_N	[0.2404075, 0.4917761]	[0.4895496, 0.7451487]	[0.4141951, 0.6786560]

		\hat{c}_N	[0.15611472, 0.3649140]	[0.11654981, 0.25334547]	[0.11588814, 0.2634528]
--	--	-------------	-------------------------	--------------------------	-------------------------

Table 4: Monte Carlo simulations conducted for the NGoE distribution

$a_N = [1, 1.4], \quad b_N = [1, 9, 2, 3], \quad c_N = [1, 2, 1, 6]$					
N	Est.	Est.par	MLE	LSE	WLSE
25	MEAN	\hat{a}_N	[0.5887893, 0.8450248]	[1.2683382, 1.818845]	[1.1002471, 1.7639706]
		\hat{b}_N	[0.6532317, 0.6922737]	[0.8227156, 0.8639881]	[0.8285207, 0.9008997]
		\hat{c}_N	[2.454202, 3.507773]	[1.5833120, 2.1337883]	[1.6837549, 2.2981807]
	MSE	\hat{a}_N	[0.3356610, 0.8860687]	[1.1366543, 1.885466]	[0.6343617, 6.7269729]
		\hat{b}_N	[2.5857378, 3.4819561]	[1.4364973, 2.2903394]	[1.4155124, 2.3789545]
		\hat{c}_N	[2.185217, 2.244143]	[0.5143024, 1.1948636]	[0.5763126, 1.3568801]
	RMSE	\hat{a}_N	[0.5793625, 0.9413122]	[1.0661399, 1.373123]	[0.7964683, 2.5936409]
		\hat{b}_N	[1.6080229, 1.8660000]	[1.1985396, 1.5133867]	[1.1897531, 1.5423860]
		\hat{c}_N	[1.478248, 2.244143]	[0.7171488, 1.0930982]	[0.7591526, 1.1648520]
	BAIS	\hat{a}_N	[0.4112107, 0.5549752]	[0.2683382, 0.418845]	[0.1002471, 0.3639706]
		\hat{b}_N	[1.2467683, 1.6077263]	[1.0772844, 1.4360119]	[1.0714793, 1.3991003]
		\hat{c}_N	[1.254202, 1.907773]	[0.3833120, 0.5337883]	[0.4837549, 0.6981807]
50	MEAN	\hat{a}_N	[0.6258331, 0.8269640]	[0.9998650563, 1.438732]	[0.8501036, 1.2488820]
		\hat{b}_N	[0.7794524, 0.8812508]	[0.8704179, 1.024662]	[0.8241932, 1.012648]
		\hat{c}_N	[2.252872, 3.258521]	[1.6534740, 2.2309253]	[1.8002450, 2.4260568]
	MSE	\hat{a}_N	[0.2560783, 0.5791875]	[0.3390656988, 0.677393]	[0.1971035, 0.5263080]
		\hat{b}_N	[2.8666991, 3.3844636]	[1.3326839, 2.310943]	[1.4934023, 2.241891]
		\hat{c}_N	[1.509798, 3.793955]	[0.4271573, 0.8907634]	[0.5866776, 1.2231896]
	RMSE	\hat{a}_N	[0.5060418, 0.7610437]	[0.5822934817, 0.823039]	[0.4439634, 0.7254709]
		\hat{b}_N	[1.6931329, 1.8396912]	[1.1544193, 1.520179]	[1.2220484, 1.497295]
		\hat{c}_N	[1.228739, 1.947808]	[0.6535727, 0.9438026]	[0.7659488, 1.1059790]
	BAIS	\hat{a}_N	[0.3741669, 0.5730360]	[0.0001349437, 0.038732]	[0.1498964, 0.1511180]
		\hat{b}_N	[1.1205476, 1.4187492]	[1.0295821, 1.275338]	[1.0758068, 1.287352]
		\hat{c}_N	[1.052872, 1.658521]	[0.4534740, 0.6309253]	[0.6002450, 0.8260568]
100	MEAN	\hat{a}_N	[0.6823063, 0.9370331]	[0.8639367, 1.2778272]	[0.7898588, 1.1106399]
		\hat{b}_N	[0.9928113, 1.158350]	[0.925258, 1.067742]	[0.9250837, 0.9911886]
		\hat{c}_N	[2.1053695, 2.982147]	[1.713232, 2.35818443]	[1.7906201, 2.530286]
	MSE	\hat{a}_N	[0.2640006, 0.5468129]	[0.1617537, 0.5476777]	[0.1213734, 0.2979603]
		\hat{b}_N	[2.9373780, 3.586256]	[1.3967830, 2.380464]	[1.4371578, 2.3378187]
		\hat{c}_N	[1.2383387, 1.708953]	[0.4348575, 1.0385527]	[0.5214322, 1.294769]
	RMSE	\hat{a}_N	[0.5138099, 0.7394680]	[0.4021862, 0.7400525]	[0.3483869, 0.5458574]
		\hat{b}_N	[1.7138781, 1.893741]	[1.181855, 1.542875]	[1.1988152, 1.5289927]
		\hat{c}_N	[1.1128067, 1.708953]	[0.6594372, 1.0190940]	[0.722102, 1.1378796]
	BAIS	\hat{a}_N	[0.3176937, 0.4629669]	[0.1360633, 0.1221728]	[0.2101412, 0.2893601]
		\hat{b}_N	[0.9071887, 1.141650]	[0.974741, 1.232258]	[0.9749163, 1.3088114]
		\hat{c}_N	[0.9053695, 1.382147]	[0.5132323, 0.7581844]	[0.5906201, 0.930286]
150	MEAN	\hat{a}_N	[0.7292710, 0.9644761]	[0.80159573, 1.1367403]	[0.7899820, 1.0491619]
		\hat{b}_N	[1.1213653, 1.3121687]	[1.0148973, 1.173121]	[1.0313131, 1.131217]
		\hat{c}_N	[1.9797816, 2.846402]	[1.7124537, 2.3615873]	[1.7395158, 2.5040847]
	MSE	\hat{a}_N	[0.2227591, 0.5106986]	[0.09263428, 0.2245738]	[0.1068058, 0.2460769]
		\hat{b}_N	[2.3373112, 4.1891276]	[1.2960749, 2.172796]	[1.2927321, 2.168210]
		\hat{c}_N	[1.0381192, 2.516863]	[0.4154301, 0.9564712]	[0.4608742, 1.2385615]
	RMSE	\hat{a}_N	[0.4719736, 0.7146318]	[0.30435880, 0.4738921]	[0.3268116, 0.4960613]
		\hat{b}_N	[1.5288267, 2.0467358]	[1.1384529, 1.474041]	[1.1369838, 1.472484]
		\hat{c}_N	[1.0188814, 1.586463]	[0.6445387, 0.9779934]	[0.6788772, 1.1129068]
	BAIS	\hat{a}_N	[0.2707290, 0.4355239]	[0.19840427, 0.2632597]	[0.2100180, 0.3508381]
		\hat{b}_N	[0.7786347, 0.9878313]	[0.8851027, 1.126879]	[0.8686869, 1.168783]
		\hat{c}_N	[0.7797816, 1.246402]	[0.5124537, 0.7615873]	[0.5395158, 0.9040847]

In Tables 3-4 of the NGoE distribution, three parameter estimation methods are used: the MLE method, the LSE method, and the WLSE method. Through Monte Carlo simulation, the performance of each method was evaluated based on Bias and RMSE.

1. The best way to estimate parameters:

- Based on simulation :MLE method showed better overall performance, as it had lower bias and RMSE values compared to other methods. This means that MLE provides more accurate estimates of parameters.

- Regarding sample size :When the sample size increases (eg $n=150$), the performance of MLE improves significantly, as the bias decreases and the estimates get closer to the true values of the parameters. This shows that MLE works better with large samples.
- Best parameters :In the simulation, parameters a_N , b_N , and c_N were evaluated. In general, parameters estimated using MLE showed better performance with increasing sample size. For example:
 - The parameter a_N shows good performance at large samples, where the RMSE error is significantly reduced.
 - The other parameters b_N and c_N follow the same pattern, with estimates improving as the sample size increases.
- It is clear from the simulation that the estimation accuracy improves as the sample size increases. For example, as the sample size increases from 25 to 150, the values for bias and RMSE decrease, meaning that the estimates get closer to the true values of the parameters. This suggests that the estimate is better and more stable with larger samples, as error is reduced, and accuracy is increased.

The best values for each parameter based on those metrics used in Tables 3-4 are:

- Parameter a_N (shape parameter):
 - The best interval at $n = 150$, the estimated value of a_N was in the interval $[0.4137, 0.6140]$.
 - The lowest value of RMSE was in the interval $[0.1429, 0.2463]$, which indicates that a_N is better estimated in these intervals with a large sample size.
- Parameter b_N (scale parameter):
 - The best interval at $n = 150$, the estimated value of b_N was in the interval $[0.9596, 1.1082]$.
 - The lowest value of RMSE was in the interval $[1.1385, 1.4740]$, which indicates that b_N is more stable with larger samples.
- Parameter c_N (scale parameter):
 - The best interval $n = 150$, the estimated value of c_N was in the interval $[1.0649, 1.7395]$.
 - The lowest value of RMSE was in the interval $[0.6445, 0.9779]$, indicating stability of c_N with large samples.

1. Application

We present a practical method that makes use of two distinct sources of data. The effectiveness of the Non-Gaussian error (NGoE) distribution in effectively fitting data is illustrated. The application demonstrates the advantages of NGoE and its exceptional compatibility with the data. Table 5 displays a juxtaposition of NGoE and other distributions. This process is conducted on the data that has previously been utilized.

This comparison utilizes eight metrics. The approach utilizes two statistical measures: the Kolmogorov-Smirnov statistic (KS) and the Anderson-Darling statistic (A). The analysis also takes into account the Cramér-von Mises statistic (W) together with the HQIC, BIC, AIC, and CAIC information criterion [33,34]. Furthermore, it employs the p-value derived from the Kolmogorov-Smirnov test. These metrics are frequently employed to evaluate the accuracy of the fit.

Tables 7 display the distribution of NGoE with the lowest values for AIC, CAIC, and BIC. They are compared to distribution values that do not overlap. Moreover, the statistical tests, such as the Anderson-Darling, Watson, and Kolmogorov-Smirnov tests, provide strong evidence that the distribution of the NGoE closely aligns with the observed patterns in the data.

Table 5: Comparative distributions

Distribution	CDF
Neotrosophic Beta Exponential (NBeE) (New)	$p\lambda(1 - e^{-c_N x_N}, a_N, b_N)$
Neotrosophic Kumaraswamy Exponential (NKuE) (New)	$1 - (1 - (1 - e^{-c_N x_N})^{a_N})^{b_N}$
Neotrosophic Exponential Generalized Exponential Exponential (NEGE) (New)	$(1 - (1 - e^{-c_N x_N})^{a_N})^{b_N}$
Neotrosophic Log Gamma Exponential (NLGamE) (New)	$1 - \Gamma(-b_N \log(1 - e^{-c_N x_N}), a_N)$
Neotrosophic [0,1] Nadarajah Haghighi (N[0,1] NHE) Exponential (New)	$\frac{1 - e^{1-(1+b_N(1-e^{-c_N x_N}))^{a_N}}}{1 - e^{1-(1+b_N(1-b_N))^{a_N}}}$
Neotrosophic Exponential (NE) (New)	$1 - e^{-c_N x_N}$

The Dataset

Results and discussion The measured resistance values of the sample w.r.t change in temperature from 0 to 350 K. Temperature dependence of the resistance of metallic nanowires of diameter 15 nm [35].

[0.120, 0.143], [0.139, 0.167], [0.157, 0.187], [0.186, 0.215], [0.212, 0.244], [0.240, 0.273], [0.266, 0.297], [0.291, 0.326], [0.317, 0.349], [0.342, 0.375], [0.369, 0.399], [0.394, 0.422], [0.421, 0.447], [0.441, 0.466], [0.461, 0.494]

Table 6 presents the descriptive statistics for the initial data sample, including the mean, variance, standard deviation, maximum and minimum values, as well as the range, skewness, and kurtosis.

Table 6: Descriptive statistics for the data

Var	N	Mean	SD	Median	Trimmed	Mad	Min	Max	Range	SK	KU	Se
1	15	[0.29, 0.32]	0.11	[0.29, 0.33]	[0.29, 0.32]	[0.14, 0.15]	[0.12, 0.14]	[0.46, 0.49]	[0.34, 0.35]	[-0.05, -0.01]	[-1.51, -1.47]	0.03

Table 7: Estimates of models for data I

Dist.	-2L	AIC	CAIC	BIC	HQIC
NGoE	[-12.17674, -11.95834]	[-18.35347, -17.91668]	[-16.17165, -15.73487]	[-16.22932, -15.79253]	[-18.3761, -17.93931]
NBeE	[-10.90065, -10.58674]	[-15.80129, -15.17348]	[-13.61947, -12.99167]	[-13.67714, -13.04933]	[-15.82392, -15.1961]
NKuE	[-12.07779, -11.93904]	[-18.15558, -17.87808]	[-15.97377, -15.69627]	[-16.03143, -15.75393]	[-18.17821, -17.9007]
NEGE	[-11.52827, -11.30943]	[-17.05653, -16.61886]	[-14.87472, -14.43704]	[-14.93238, -14.49471]	[-17.07916, -16.6414]
NLGamE	[-11.87702, -11.72723]	[-17.75405, -17.45446]	[-15.57223, -15.27264]	[-15.62989, -15.3303]	[-17.77667, -17.4770]
N[0,1] NHE	[-5.344676, -6.582523]	[-7.161656, -4.686541]	[-4.979837, -2.504723]	[-5.037505, -2.562391]	[-7.184282, -4.70916]
NE	[-3.54744, -2.079019]	[-5.09488, -2.158039]	[-4.787188, -1.850347]	[-4.38683, -1.449989]	[-5.102422, -2.16558]

Table 7 compares various statistical models based on several goodness-of-fit metrics, which include:

- NGoE Distribution: This model has the best fit, as evidenced by the lowest values across most criteria. The -2L value ranges between -12.17 and -11.96, and the AIC values are the lowest at -18.35 to -17.92, meaning that this model has the best trade-off between fit and complexity.
- Other Models (NBeE, NKuE, NEGE, NLGamE, etc.): These models also provide a decent fit but perform worse than the NGoE model. For instance, the NBeE model has a higher AIC value (-15.80 to -15.17) compared to the NGoE, indicating a weaker fit to the data.
- Comparison: NGoE consistently shows the best values across all metrics, followed by NKuE and NEGE. This implies that NGoE is the most effective model in fitting this particular dataset.

Table 8: Evaluate statistical metrics for the data

Dist.	W	A	K-S	p-value
NGoE	[0.02926074, 0.03618808]	[0.2222064, 0.2677006]	[0.1042987, 0.09041123]	[0.9909796, 0.9986026]
NBEE	[0.0743582, 0.07801139]	[0.4872085, 0.5009272]	[0.15684880, 0.1657986]	[0.7451206, 0.8008947]
NKuE	[0.0308056, 0.03082524]	[0.2312379, 0.2414818]	[0.1013803, 0.1043238]	[0.990955, 0.993514]
NEGE	[0.04707363, 0.05000038]	[0.3351342, 0.3423613]	[0.1162705, 0.1184103]	[0.9680401, 0.9728294]
NLGamE	[5.39023, 5.409017]	[30.45235, 30.45588]	[0.9633316, 0.9670168]	0
Ne[0,1] NHE	[0.03044801, 0.03074176]	[0.230287, 0.2389234]	[0.2612947, 0.2883124]	[0.1345112, 0.2158392]
NE	[0.03765638, 0.03840122]	[0.2749972, 0.2807644]	[0.3384853, 0.3601381]	[0.03005951, 0.04903951]

Table 8 evaluates the fit of the different models using statistical tests such as:

- Cramér-von Mises Statistic (W): This statistic measures the goodness of fit for a distribution. Lower values indicate a better fit. The NGoE model has the lowest W values (0.029 to 0.036), suggesting a good match between the empirical and fitted distributions.
- Anderson-Darling Statistic (A): This test gives more weight to the tails of the distribution. The NGoE model also has lower A values (0.222 to 0.267), indicating a strong fit, especially in the tails.
- Kolmogorov-Smirnov (K-S) Statistic: This test compares the empirical cumulative distribution function with the model's cumulative distribution function (CDF). The NGoE model has the lowest K-S values (0.10), indicating the best fit in terms of matching the distribution's cumulative behavior.
- p-value: A high p-value suggests that the observed data fits well with the model's predicted distribution. The NGoE model shows very high p-values (~0.99), further confirming its strong performance in fitting the data.

Overall, Table 8 demonstrates that the NGoE model outperforms the other models in all goodness-of-fit tests, confirming its

superior performance.

Table 9: parameter estimators by MLE for the data

Dist.	\hat{a}_N	\hat{b}_N	\hat{c}_N
NGoE	[1.1949456, 1.387636]	[24.937512, 33.1436640]	[0.2593868, 0.326928]
NBEE	[82.0012179, 95.3493720]	[0.2027687, 0.2482111]	[27.5180937, 33.1276678]
NKuE	[3.814811, 4.714791]	[14.075968, 16.541580]	[2.007792, 2.375847]
NEGE	[3.09699, 3.103515]	[8.921518, 11.95487]	[3.09699, 3.103515]
NLGamE	[6.284694, 7.646387]	[2.715127, 3.007349]	[7.938900, 7.970714]
Ne[0,1] TEEE	[0.009278226, 0.01000018]	[-0.934937523, -0.93539246]	[6.117393795, 6.58898339]
NE	---	---	[3.122398, 3.443526]

Table 9 provides the MLE parameter estimates for each model. The parameters (a_N , b_N , and c_N) are specific to each distribution and reflect the best fit obtained through the MLE process.

- NGoE: The parameters estimated for the NGoE model are $a_N = [1.19, 1.39]$, $b_N = [24.94, 33.14]$, and $c_N = [0.26, 0.33]$. These values represent the shape, scale, and location parameters that allow the NGoE model to fit the data well.
- Other Models: For instance, NBEE has much larger a_N values (82.00 to 95.35), which suggests it requires more extreme values to fit the data, while b_N values are much smaller. The large discrepancy between these parameters indicates that other models require more drastic adjustments to fit the data, potentially leading to overfitting or poor generalization.
- The parameter estimates provide insight into the flexibility of each model in capturing the data's behavior, with the NGoE model again showing the most reasonable and reliable estimates.

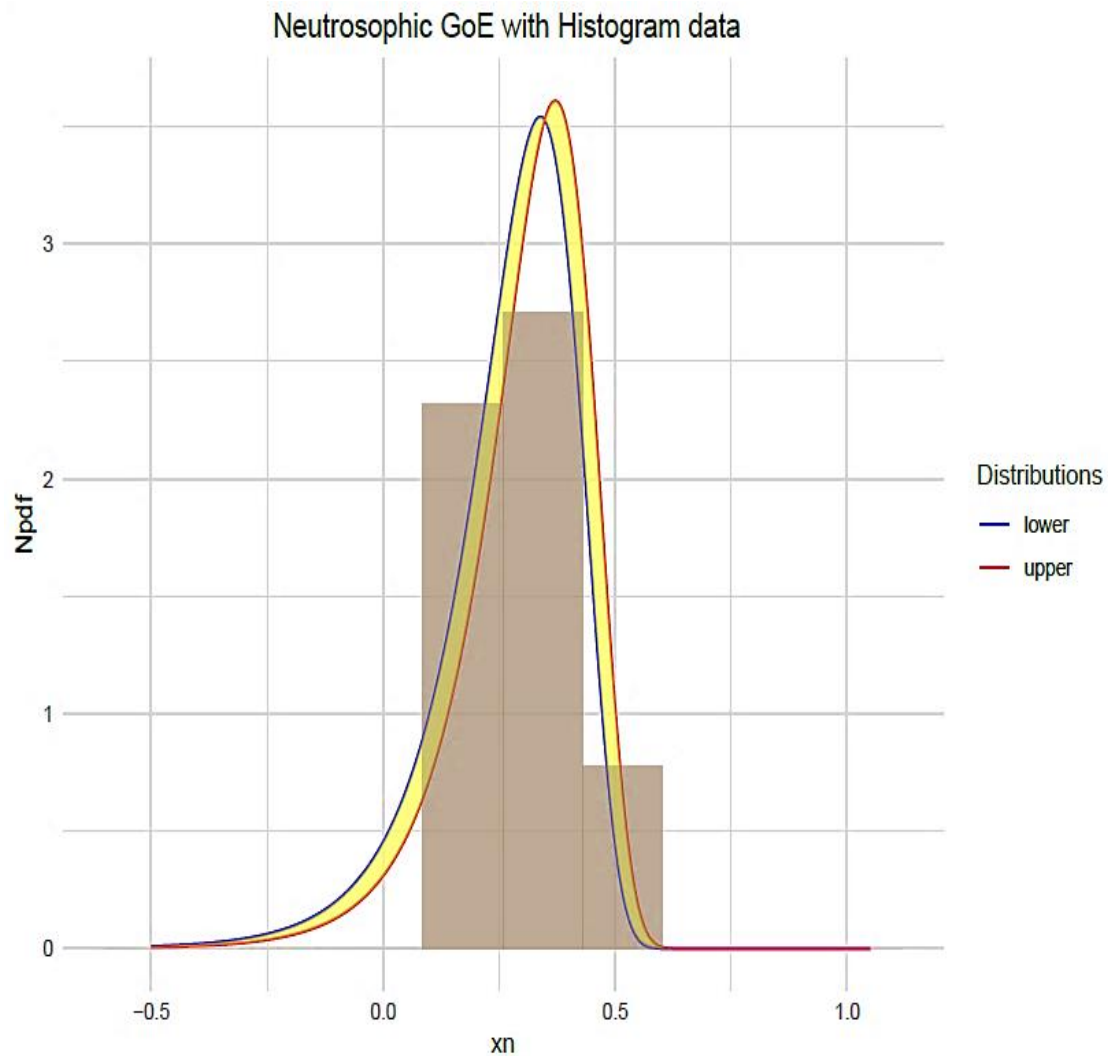


Figure 7: Fitting pdfs NGoE with histogram data set

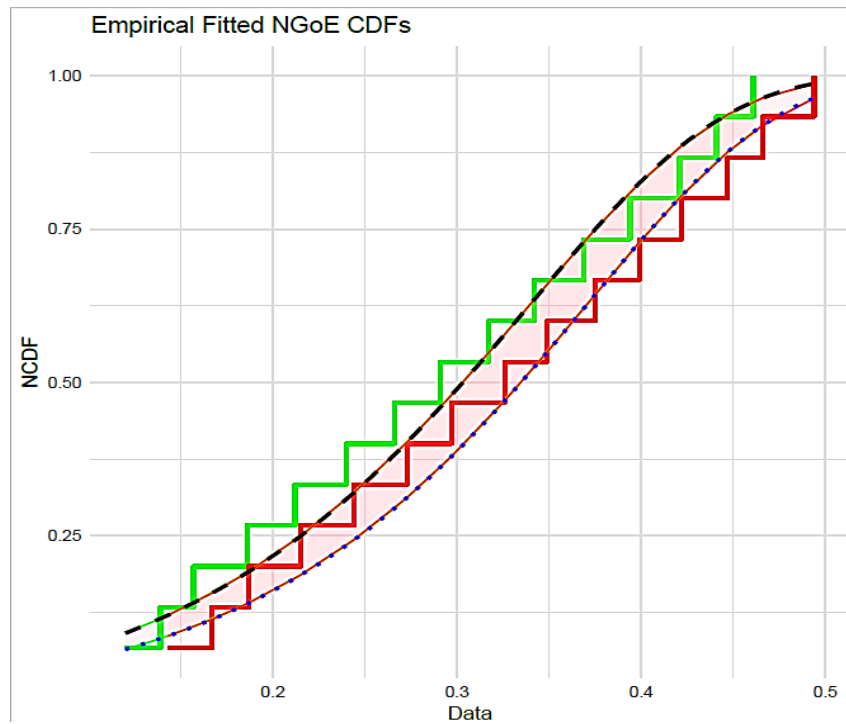


Figure 8: Empirical Fitted CDFs NGoE with histogram data set

Figure 7 provides a visual representation of the fitted neutrosophic probability density function for the NGoE model compared to the empirical data histogram. The curve represents the NGoE model's fitted distribution, while the histogram shows the actual data distribution.

- **Interpretation:** The close alignment of the NGoE curve with the histogram demonstrates that the NGoE model provides a highly accurate fit to the observed data. Areas where the curve and histogram match particularly well indicate that the model captures both the central tendency and variability of the data accurately.
- **Importance:** This figure is important because it visually confirms the results from the statistical tests in Tables 7-8, showing that the NGoE distribution accurately describes the data.

Figure 8 presents the empirical cumulative distribution function (CDF) for the NGoE model, overlaid on the empirical data's CDF.

- **Interpretation:** The NGoE's CDF closely follows the empirical CDF, indicating that the model is a good representation of the cumulative behavior of the data. The CDF is particularly useful in showing how well the model captures the overall distribution, not just the central values.
- **Importance:** A strong match between the empirical and fitted CDFs confirms that the model is effective in predicting probabilities and cumulative behavior, which is essential for applications that rely on distributional assumptions.

Conclusions

This study introduces a new family based on neutrosophic logic, with a new probabilistic model, the NGoE distribution, was derived with a neutrosophic random variable and three neutrosophic parameters. The NGoE model effectively addresses real data ambiguity by incorporating truth, indeterminacy, and falsity components directly into distribution's structure. This tri-level uncertainty representation provides greater interpretability and flexibility than traditional distribution or fuzzy models, which typically capture uncertainty in a single dimension. As a result, the neutrosophic framework better than reflects the incomplete, imprecise, and conflicting information common in engineering, reliability, and risk data.

Empirical analysis demonstrates the superiority of NGoE model over existing distributions, as reflected in lowest AIC, BIC, and KS values, indicating a more accurate fit and stronger generalization ability. The visual comparisons of Npdfs and NCDFs further confirm its consistency in capturing both control and tail behaviors of the data.

The neutrosophic modeling approach thus offers a conceptually transparent and mathematically robust mechanism for managing uncertainty bridging the gap between classical probability and fuzzy logic. It provides interpretable outputs through interval-based estimation, allowing analysts to quantify uncertainty ranges rather than single-point estimates.

Nevertheless, the current study is limited by the scope of its real data applications and the reliance on classical estimation techniques. Future research should extend practical validation across broader datasets, perform sensitivity analyses, and explore Bayesian and regression-based neutrosophic estimators to enhance computational efficiency and interpretive depth.

Authors' Contributions:

Authors have worked equally to write and review the manuscript.

Data Availability Statement:

The data that supports the findings of this study are available within the article.

Conflicts of Interest:

The authors declare no conflict of interest.

References

1. Alzaatreh, A., Lee, C., & Famoye, F. (2013). A new method for generating families of continuous distributions. *Metron*, 71(1), 63–79.
2. Tahir, M. H., et al. (2020). A new Kumaraswamy generalized family of distributions with properties, applications, and bivariate extension. *Mathematics*, 8(11), 1989.
3. Hussain, S., et al. (2022). The generalized alpha exponent power family of distributions: Properties and applications. *Mathematics*, 10(9), 1421.
4. Agu, F. I., Eghwerido, J. T., & Nziku, C. K. (2022). The alpha power Rayleigh-G family of distributions. *Mathematica Slovaca*, 72(4), 1047–1062.
5. Noori, N. A., Khalaf, A. A., & Khaleel, M. A. (2024). A new generalized family of odd Lomax-G distributions: Properties and applications. *Advances in the Theory of Nonlinear Analysis and Its Application*, 7(4), 1–16. <https://doi.org/10.17762/atnaa.v.i.278>
6. Muhammad, M., Liu, L., Abba, B., Muhammad, I., Bouchane, M., Zhang, H., & Musa, S. (2023). A new extension of the Topp–Leone family of models with applications to real data. *Annals of Data Science*, 10(1), 225–250.
7. Alanaz, M. M., Mustafa, M. Y., & Algamal, Z. Y. (2023). Neutrosophic Lindley distribution with application for alloying metal melting point. *Full Length Article*, 21(4), 65–75.
8. Algamal, Z. Y., et al. (2024). Neutrosophic Beta-Lindley distribution: Mathematical properties and modeling bladder cancer data. *Full Length Article*, 23(2), 186–196.
9. Alanaz, M. M., & Algamal, Z. Y. (2023). Neutrosophic exponentiated inverse Rayleigh distribution: Properties and applications. *International Journal of Neutrosophic Science*, 21(4), 36–43.
10. Al-Saqal, O. E., Hadied, Z. A., & Algamal, Z. Y. (2025). Modeling bladder cancer survival function based on neutrosophic inverse Gompertz distribution. *International Journal of Neutrosophic Science*, 1, 75–85.
11. Hammood, N. M., Rashad, N. K., & Algamal, Z. Y. (2025). Neutrosophic Topp-Leone extended exponential distribution modeling with application for bladder cancer patients. *International Journal of Neutrosophic Science*, 1, 239–249.
12. Mustafa, M. Y., & Algamal, Z. Y. (2023). Neutrosophic inverse power Lindley distribution: Modeling and application for bladder cancer patients. *Full Length Article*, 21(2), 216–226.
13. Zeina, M. B., & Hatip, A. (2021). Neutrosophic random variables. *Neutrosophic Sets and Systems*, 39, 44–52.
14. Norouzirad, M., Rao, G. S., & Mazarei, D. (2023). Neutrosophic generalized Rayleigh distribution with application. *Neutrosophic Sets and Systems*, 58(1), 15–25.
15. Alzaatreh, A., Lee, C., & Famoye, F. (2013a). A new method for generating families of continuous distributions. *Metron*, 71(1), 63–79.
16. Alexander, C., Cordeiro, G. M., Ortega, E. M. M., & Sarabia, J. M. (2012). Generalized beta-generated distributions. *Computational Statistics & Data Analysis*, 56, 1880–1897.
17. Ristić, M. M., & Balakrishnan, N. (2012). The gamma-exponentiated exponential distribution. *Journal of Statistical Computation and Simulation*, 82, 1191–1206.
18. Alzaghal, A., Lee, C., & Famoye, F. (2013). Exponentiated T-X family of distributions with some applications. *International Journal of Probability and Statistics*, 2, 31–49.
19. Torabi, H., & Montazari, N. H. (2014). The logistic-uniform distribution and its application. *Communications in Statistics – Simulation and Computation*, 43, 2551–2569.
20. Khalaf, A. A., Ibrahim, M. Q., & Noori, N. A. (2024). [0,1] Truncated exponentiated exponential Burr type X distribution with applications. *Iraqi Journal of Science*, 4428–4440.
21. Tahir, M. H., Cordeiro, G. M., Alizadeh, M., Mansoor, M., Zubair, M., & Hamedani, G. G. (2015). The odd generalized exponential family of distributions with applications. *Journal of Statistical Distributions and Applications*, 2(1), 1–28.
22. Ahmad, Z., Elgarhy, M., & Hamedani, G. G. (2018). A new Weibull-X family of distributions: Properties, characterizations and applications. *Journal of Statistical Distributions and Applications*, 5, 1–18.
23. Ahmad, A., Lone, M. A., & Rather, A. A. (2024). EJAZ distribution: A new two-parametric distribution for modeling data. *Reliability: Theory & Applications*, 19(1[77]), 191–201.
24. Merovci, F., et al. (2016). The beta Burr type X distribution: Properties with application. *SpringerPlus*, 5, 1–18.
25. Noori, N. A. (2023). Exploring the properties, simulation, and applications of the odd Burr XII Gompertz distribution. *Advances in the Theory of Nonlinear Analysis and Its Application*, 7(4), 60–75.

26. Khalaf, A. A., Noori, N., & Khaleel, M. (2024). A new expansion of the inverse Weibull distribution: Properties with applications. *Iraqi Statisticians Journal*, 52–62.
27. Song, Y., et al. (2020). A hybrid statistical data-driven method for on-line joint state estimation of lithium-ion batteries. *Applied Energy*, 261, 114408.
28. Almetwally, E. M. (2022). The odd Weibull inverse Topp–Leone distribution with applications to COVID-19 data. *Annals of Data Science*, 9(1), 121–140.
29. Mehmood, T., Sæbø, S., & Liland, K. H. (2020). Comparison of variable selection methods in partial least squares regression. *Journal of Chemometrics*, 34(6), e3226.
30. Noori, N. A., & Mohammad, A. A. (2021). Dynamical approach in studying GJR-GARCH (Q, P) models with application. *Tikrit Journal of Pure Science*, 26(2), 145–156.
31. Abd El-Latif, A. M., Almulhim, F. A., Noori, N. A., Khaleel, M. A., & Alsaedi, B. S. (2025). Properties with application to medical data for new inverse Rayleigh distribution utilizing neutrosophic logic. *Journal of Radiation Research and Applied Sciences*, 18(2), 101391.
32. Jumaa, M. H., Qaddoori, A. S., Khalaf, S. A., Noori, N. A., & Khaleel, M. A. (2025). Mathematical properties and simulations of the neutrosophic Gompertz-inverse Burr-X distribution with application to under-five mortality. *Iraqi Journal for Computer Science and Mathematics*, 6(3), 23.
33. Husain, Q. N., Qaddoori, A. S., Noori, N. A., Abdullah, K. N., Suleiman, A. A., & Balogun, O. S. (2025). New expansion of Chen distribution according to the neutrosophic logic using the Gompertz family. *Manuscript in preparation*.
34. Noori, N. A., Khaleel, M. A., Khalaf, S. A., & Dutta, S. (2025). Analytical modeling of expansion for odd Lomax generalized exponential distribution in framework of neutrosophic logic: A theoretical and applied study on neutrosophic data. *Manuscript in preparation*.
35. Elguindi, J., Wagner, J., & Rensing, C. (2009). Genes involved in copper resistance influence survival of *Pseudomonas aeruginosa* on copper surfaces. *Journal of Applied Microbiology*, 106, 1448–1455.

© 2026 by the authors. **Disclaimer / Publisher's Note:** The views, opinions, and data presented in all published content are solely those of the individual authors and contributors. They do not necessarily reflect the positions of Sphinx Scientific Press (SSP) or its editorial team. SSP and the editors disclaim any responsibility for harm or damage to individuals or property that may result from the use of any information, methods, instructions, or products mentioned in the content.

